

Thermo-Calc  
Software

# TC-Prisma Online Training Course

*Day 2 – April 24, 2024*

*Åke Jansson, Qing Chen*

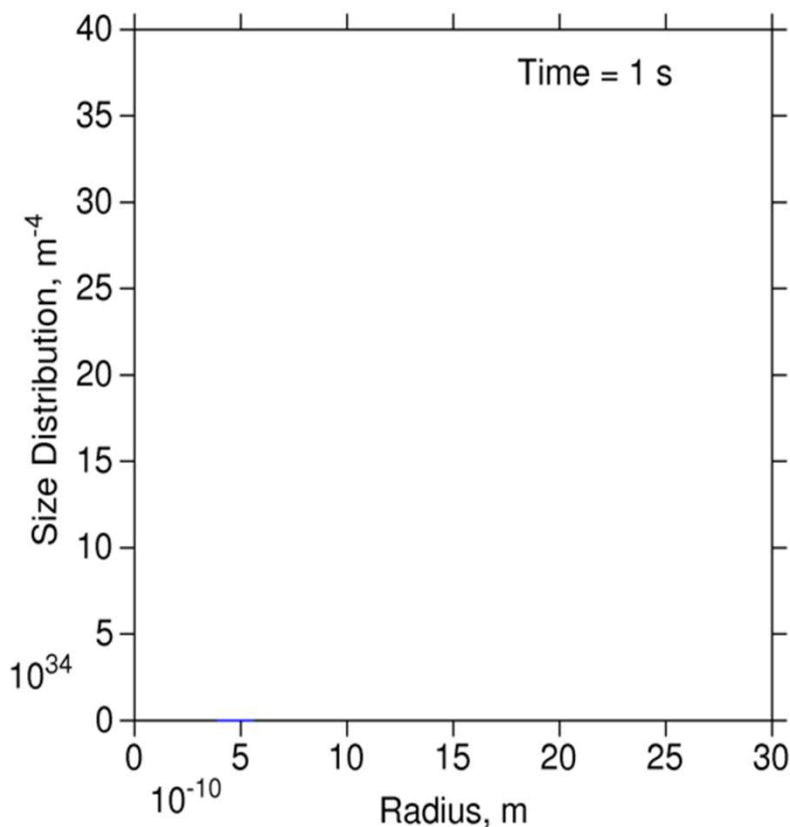


# Theory: Growth

# Models and Model Parameters



LS (Langer-Schwartz) and KWN (Kampmann and Wagner Numerical) Approach



Continuity equation

$$\frac{\partial f(r, t)}{\partial t} = -\frac{\partial}{\partial r} [v(r)f(r, t)] + j(r, t)$$

Mass balance

$$C_0^\alpha = C^\alpha + (C^\beta - C^\alpha) \int_0^\infty \frac{4\pi}{3} f(r, t) r^3 dr$$

# Models: Growth Rate



## Available models

### Binary

$$v = \frac{c^\alpha - c^{\alpha/\beta}(r) D}{c^\beta - c^{\alpha/\beta}(r)} \frac{D}{r}$$

H.B. Aaron, D. Fainstain, G. R. Kotler,  
J. Appl. Phys., 41(1970)4404

### Multi-Component Coarsening

$$v = \frac{2\sigma V_m^\alpha}{(\Delta C^{\alpha\beta}) [M]^{-1} (\Delta C^{\alpha\beta})} \frac{1}{r} \left( \frac{1}{r^*} - \frac{1}{r} \right)$$

J.E. Morral, G.R. Purdy, Scripta  
Metall. Mater., 30(1994)905-908

### PrecipiCalc Model

$$v = \left( 1 + r \sqrt{4\pi N_v r_a} \right) \frac{\Delta \bar{c}_i G_{ij}^\alpha \Delta c_j^\infty + \bar{c}_\delta^\beta (\bar{\mu}_\delta^\alpha - \bar{\mu}_\delta^\beta) - 2V_m^\beta \sigma / r}{r \Delta \bar{c}_i G_{ij}^\alpha D_{jk}^{-1} B_k + 1/M}$$

H.J. Jou et al. Superalloy 2004, p.877-886

# Models: Growth Rate



## Available models

- Similarity-Supersaturation

$$v = \frac{S_1 \sqrt{D_1}}{2\sqrt{t}} = \frac{S_2 \sqrt{D_2}}{2\sqrt{t}} = \dots \quad S_i = f(\Omega_i)$$

T.Sourmail, Ph. D Thesis, Univ. Cambridge, 2002

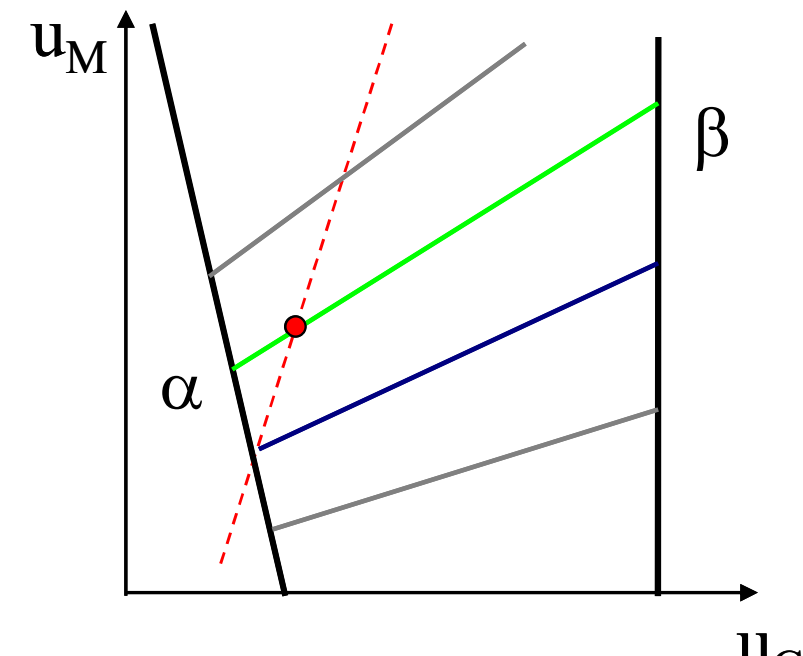
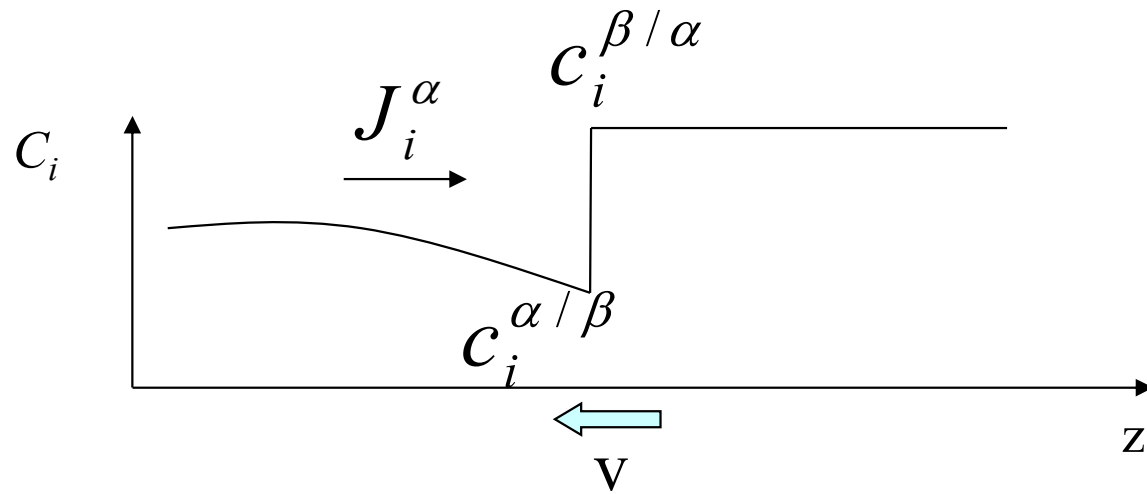
- Thermodynamic Extremum Principle

$$\dot{\rho}_k = \frac{F - (2\gamma_k/\rho_k)}{RT\rho_k} \left[ \sum_{i=1}^n \frac{(c_{ki} - c_{0i})^2}{c_{0i}D_{0i}} \right]^{-1}$$

Svoboda J, Fischer FD, Fratzl P, Kozeschnik E. Mater Sci Eng A, 385(2004)166

# Models: Growth Rate

- Local equilibrium at interface
- Flux balance equation



$$\mu_i^{\alpha/\beta} = \mu_i^{\beta/\alpha}$$

$$v(c_i^{\beta/\alpha} - c_i^{\alpha/\beta}) = -J_i^\alpha = \sum_j D_{ij}^\alpha \frac{\partial c_j^\alpha}{\partial z}$$

# Models: Growth Rate



Q. Chen, J. Jeppsson, J. Ågren, Acta Mater. 56(2008)1890-1896

## Advanced – Analytical Flux-balance Approximation

$$\mu_i^{\alpha/\beta} = \mu_i^{\beta/\alpha} + \frac{2\sigma V_m^\beta}{r}$$
$$v(c_i^{\beta/\alpha} - c_i^{\alpha/\beta}) = c_i^{\alpha/\beta} M_j (\mu_i^\alpha - \mu_i^{\alpha/\beta}) / \xi_i r$$

Cross diffusion      High supersaturation

## General model – new in TC 2019a

$$v = \frac{K}{r} \left( \Delta G_m - \frac{2\sigma V_m}{r} \right)$$

# Models: Growth Rate



General & Simplified –  
different expressions for  $K$

$$v = \frac{K}{r} \left( \Delta G_m - \frac{2\sigma V_m}{r} \right)$$

**Simplified**

Similar atomic  
mobilities

$$K_{sphere}^{simplified} = \left[ \sum_i \frac{\left( X_i^{\beta/\alpha}(r) - X_i^{\alpha/\beta}(r) \right)^2 \xi_i}{X_i^{\alpha/\beta}(r) M_i} \right]^{-1}$$

Number fixed  
Coarsening

**General**

Very different  
atomic  
mobilities

$$K_{sphere}^{Morral-Purdy} = \left[ (\Delta X^{\alpha\beta}) [M]^{-1} (\Delta X^{\alpha\beta}) \right]^{-1}$$

Volume fixed  
Coarsening

**General**

Very different  
atomic  
mobilities

$$K_{sphere}^{general} = \left[ (\Delta X^{\alpha\beta}) [\ddot{G}] [\bar{D}]^{-1} (\Delta X^{\alpha\beta}) \right]^{-1}$$

Volume fixed  
Growth

# Models: Growth Rate



## Para-equilibrium and Non-partitioning local equilibrium

$$v = \frac{K^{PE/NPLE}}{r} \left( \Delta G_m^{PE/NPLE} - \frac{2\sigma V_m}{r} \right)$$

$$K_{sphere}^{PE/NPLE} = \left[ \sum_i \frac{\left( u_C^{\beta/\alpha}(r) - u_C^{\alpha/\beta}(r) \right)^2 \xi_C}{u_C^{\alpha/\beta}(r) M_C} \right]^{-1}$$

$$\beta^* = \frac{4\pi r^2 K}{a^4}$$

# Models: NPLE and Para-eq.

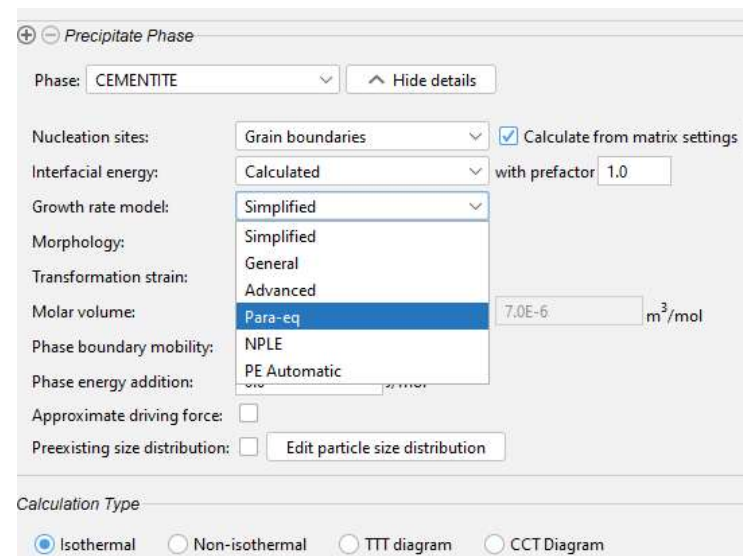


Models to handle NPLE (non partitioning local equilibrium) and para-equilibrium were introduced several years ago.

These models deal with fast diffusion processes and are additions to the Simplified growth rate model.

These models need only to consider the movement of the fast diffusing specie, usually an interstitial such as C or N.

The new (2023) **PE Automatic** model enables a smooth transition from Paraequilibrium growth rate model to Simplified growth rate model. The rate of transition process is dependent on the relative differences in diffusion between C and substitutional elements, as well as the differences in driving force between PE and Ortho-Equilibrium (i.e. Local Eq.).



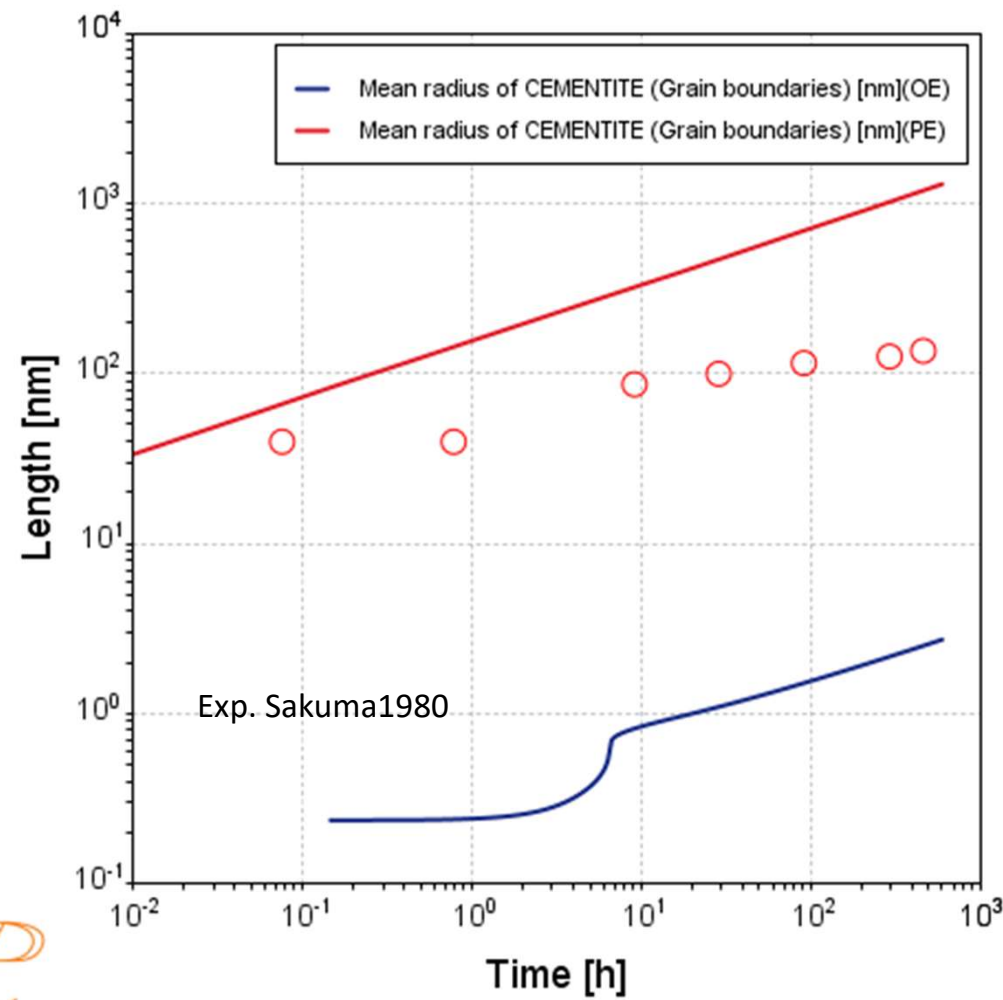
## The non-zero volume correction

$$v' = v \left( 1 + r \sqrt{4\pi N_V \langle r \rangle} \right)$$

Chen MK, Voorhees PW, Modeling and simulation in materials science and engineering 1993;1:591-612.

# Ortho-eq vs Para-eq

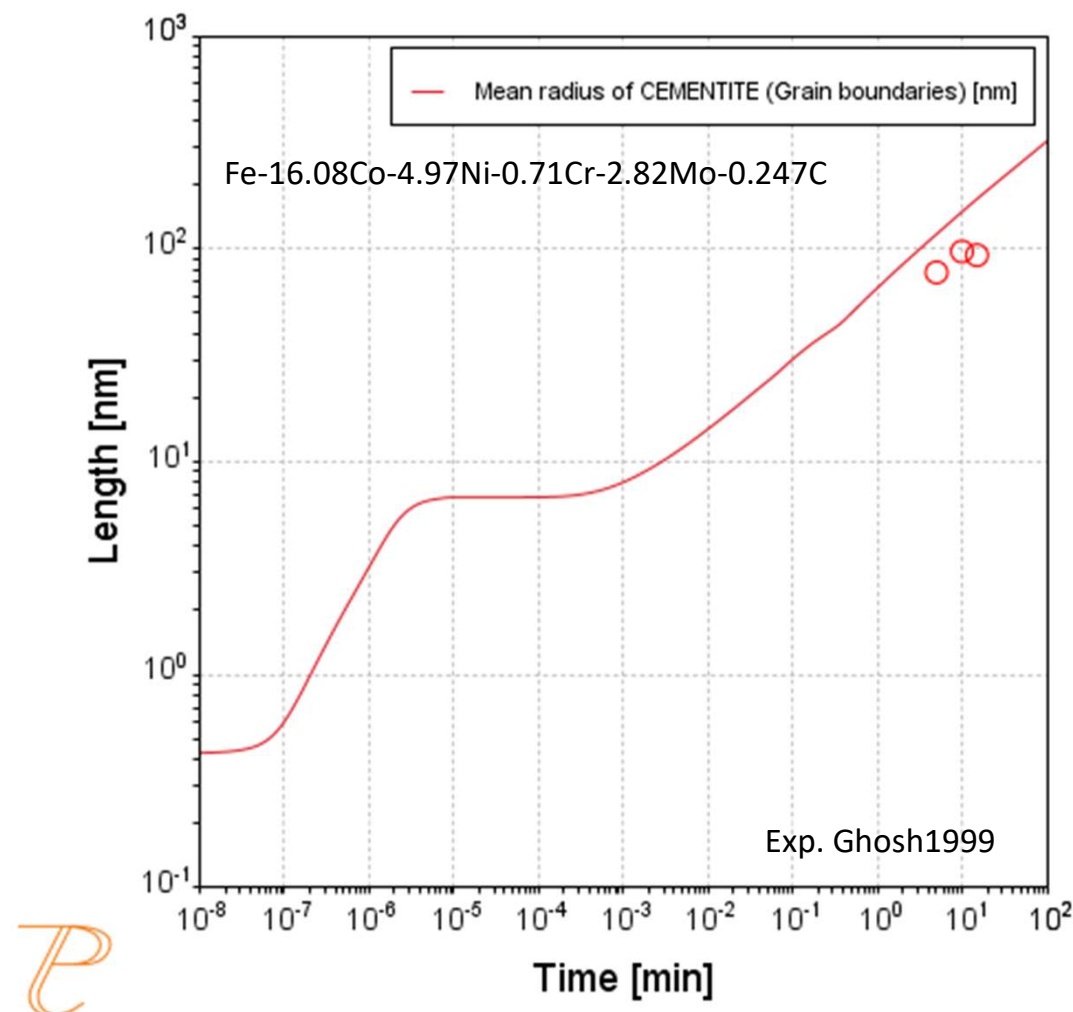
Fe-0.26C-0.11Cr at T= 773 K



P

# Ortho-eq vs Para-eq

Ultra-high-strength steel at T= 783 K



P

# Precipitate Shapes

## ➤ Interfacial Energy Anisotropy\*

$$\frac{\sigma_l}{\sigma_r} = \frac{l}{r} = \alpha$$

## ➤ Elastic Strain Energy

- Elastically Isotropic or Cubic Systems
- First Approximation: Elastically Homogenous
- Eshelby's Theory\*\*

## ➤ Particle Shape

- Determined by Minimization of Combined Interfacial Energy and Elastic Energy
- User-Defined, Fixed Value

Needle  
(Prolate Spheroid)

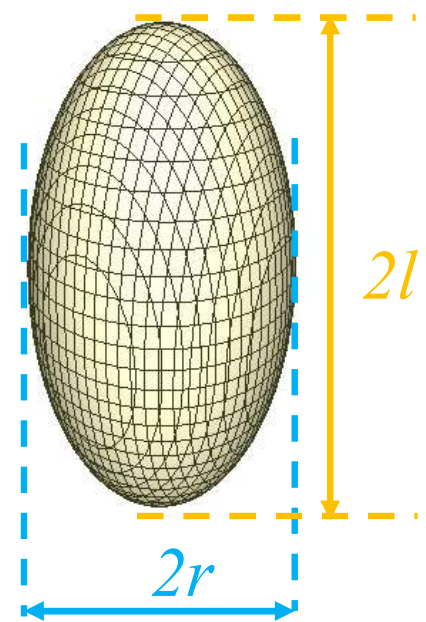
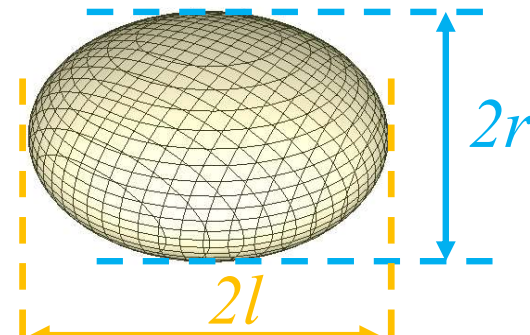


Plate  
(Oblate Spheroid)



\* C.A. Johnson, *Surf. Sci.* 3(1965)429

\*\* J.D. Eshelby, *Proc. Roy. Soc. A*, 241(1957)376

# Effect on Growth Rate

K. Wu, Q. Chen, P. Mason, J Phase Eq. Diffus. 39(2018)571-583.

$$\frac{dR}{dt} = K_\sigma \cdot K_{\text{shp}} \cdot \left( \frac{dR}{dt} \right)_{\text{sph}}$$

R: Radius of Equivalent Sphere

## ➤ Interfacial energy anisotropy\*

- Generalized Gibbs-Thomson Effect

$$\mu(R) - \mu(\infty) = K_\sigma \frac{2\sigma_{\text{ch}}^{\text{sp}} V_m}{R}$$

## ➤ Shape Effect

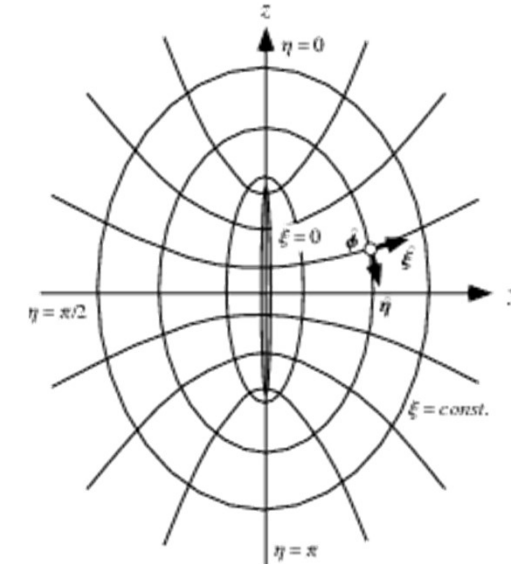
- Assumption of Shape Conserving Concentration Field\*\*

\* C.A. Johnson, *Surf. Sci.* 3(1965)429

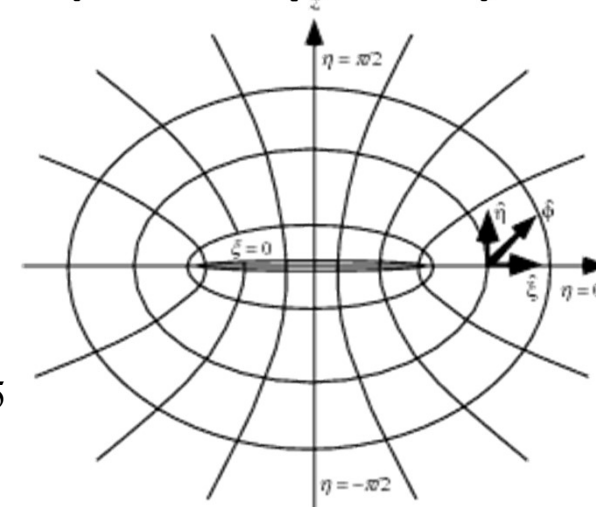
\*\* F.S. Ham, *Quart. Appl. Math.*, 17(1959)137; *J Phys. Chem. Solids*, 6(1958)335

\*\*\* <http://mathworld.wolfram.com>

Needle\*\*\*  
(Prolate Spheroid)



Plate\*\*\*  
(Oblate Spheroid)



# Effect on Growth Rate



K. Wu, Q. Chen, P. Mason, J Phase Eq. Diffus. 39(2018)571-583.

$$\frac{dR}{dt} = K_\sigma \cdot K_{\text{shp}} \cdot \left( \frac{dR}{dt} \right)_{\text{sph}}$$

R: Radius of Equivalent Sphere

Aspect ratio

$$\alpha = \frac{l}{r} \geq 1$$

Eccentricity

$$e = \sqrt{1 - \frac{1}{\alpha^2}}$$

## Needle

$$K_\sigma = \sqrt[3]{\alpha}$$

$$K_{\text{shp}} = \frac{2\sqrt[3]{\alpha^2}e}{\ln(1+e) - \ln(1-e)}$$

$\alpha$	$K_\sigma K_{\text{shp}}$
10.0	3.3
15.0	4.4
20.0	5.4

## Plate

$$K_\sigma = \sqrt[3]{\alpha^2}$$

$$K_{\text{shp}} = \frac{e\sqrt[3]{\alpha}}{\arccos(0) - \arccos(e)}$$

$\alpha$	$K_\sigma K_{\text{shp}}$
10.0	6.8
15.0	10.0
20.0	13.1

# Examples

## Ni alloys

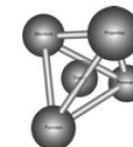
# TC-PRISMA Example



Available online at [www.sciencedirect.com](http://www.sciencedirect.com)



Acta Materialia 56 (2008) 448–463



Acta MATERIALIA

[www.elsevier.com/locate/actamat](http://www.elsevier.com/locate/actamat)

## Effects of a tungsten addition on the morphological evolution, spatial correlations and temporal evolution of a model Ni–Al–Cr superalloy

Chantal K. Sudbrack<sup>a,b</sup>, Tiffany D. Ziebell<sup>a,c</sup>, Ronald D. Noebe<sup>d</sup>, David N. Seidman<sup>a,e,\*</sup>

<sup>a</sup> Department of Materials Science and Engineering, Northwestern University, 2220 Campus Drive, Evanston, IL 60208, USA

<sup>b</sup> Materials Science Division, Argonne National Laboratory, Argonne, IL 60439, USA

<sup>c</sup> Department of Materials Science and Engineering, Massachusetts Institute of Technology, 77 Massachusetts Avenue, Cambridge, MA 02139, USA

<sup>d</sup> NASA Glenn Research Center, 21000 Brookpark Road, Cleveland, OH 44135, USA

<sup>e</sup> Northwestern University Center for Atom-Probe Tomography, 2220 Campus Drive, Evanston, IL 60208, USA

Received 8 July 2007; received in revised form 26 September 2007; accepted 28 September 2007

Available online 26 November 2007

---

### Abstract

The effect of adding 2 at.% W to a model Ni–Al–Cr superalloy on the morphological evolution, spatial correlations and temporal evolution of  $\gamma'$ (L1<sub>2</sub>)-precipitates at 1073 K is studied with scanning electron microscopy and atomic force microscopy. Adding W yields a larger microhardness, earlier onset of spheroidal-to-cuboidal precipitate morphological transition, larger volume fraction (from ~20% to 30%), reduction in coarsening kinetics by one-third and a larger number density ( $N_v$ ) of smaller mean radii ( $\langle R \rangle$ ) precipitates. The kinetics of  $\langle R \rangle$  and interfacial area per unit volume obey  $t^{1/3}$  and  $t^{-1/3}$  relationships, respectively, which is consistent with coarsening driven by interfacial energy reduction. The  $N_v$  power-law dependencies deviate, however, from model predictions, indicating that a stationary state is not achieved. Quantitative analyses with precipitate size distributions, pair correlation functions and edge-to-edge inter-precipitate distance distributions give insight into two-dimensional microstructural evolution, including the elastically driven transition from a uniform  $\gamma'$ -distribution to one-dimensional  $\langle 001 \rangle$ -strings to eventually clustered packs of  $\gamma'$ -precipitates in the less densely packed Ni–Al–Cr alloy.

© 2007 Acta Materialia Inc. Published by Elsevier Ltd. All rights reserved.

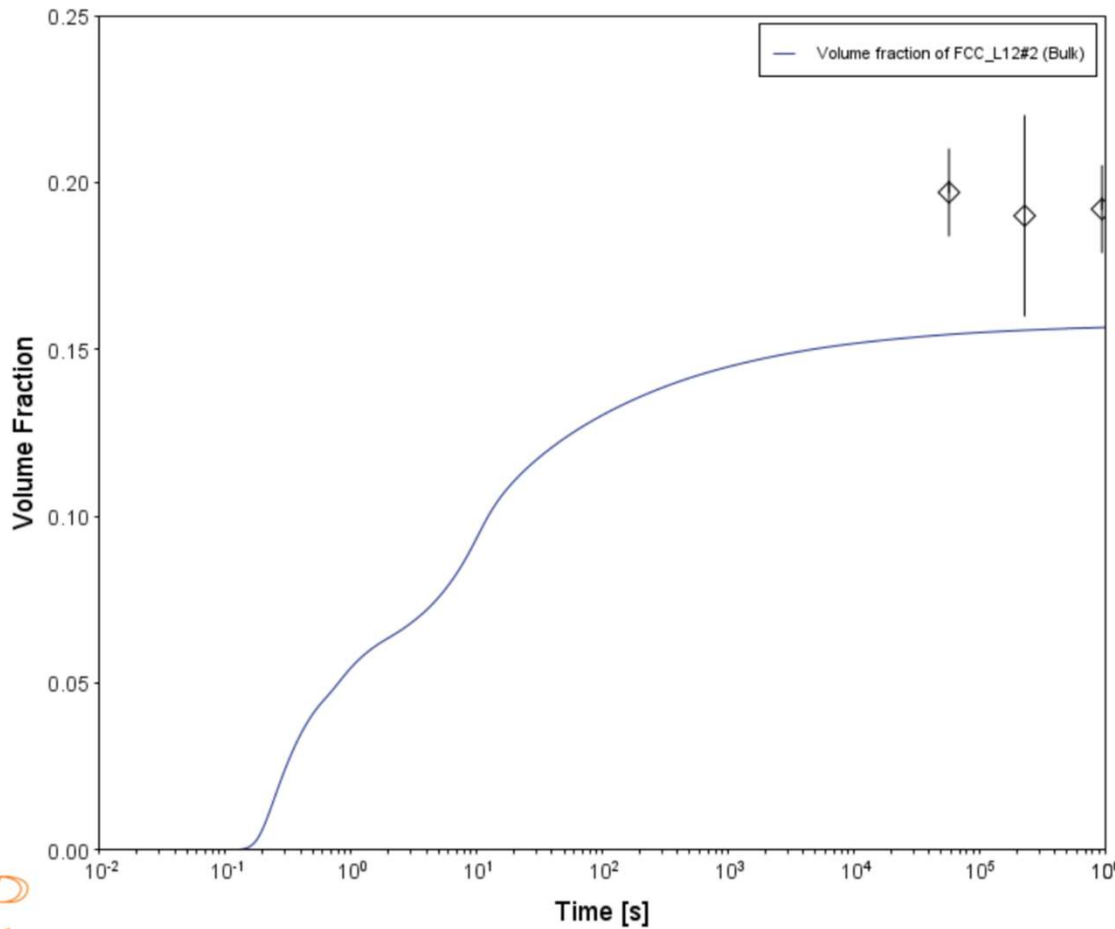
# TC-PRISMA Example 1



System	
Database package	TCNI12 + MOBNI6
Elements	Ni, Al, Cr
Matrix phase	DIS_FCC_A1
Precipitate phases	FCC_L12#2
Conditions	
Composition	Ni – 9.8 Al – 8.3 Cr (at.%)
Temperature	800 °C
Simulation time	1E6 s
Nucleation properties	Nucleation Site Type: Bulk
Data Parameters – Interfacial Energies	
Interfacial Energy	Calculated
Molar Volume (Matrix phase):	DIS_FCC_A1: from database
Molar Volume (Precipitate phase):	FCC_L12#2: from database

# TC-PRISMA Example 1

Strange result for Volume fraction compared with experimental data from Sudbrack when the setup on previous page is used:



Results				
	Volume fraction	Number density	Mean radius	Table renderer 1
<b>System</b>				
Moles	1.00000			
Mass	55.02701	[g]		
Temperature	1073.15000	[K]		
Total Gibbs Energy	-66916.16735	[J]		
Enthalpy	-51528.57953	[J]		
Volume	6.97148E-6	[m <sup>3</sup> ]		
<b>Component</b>				
Al	0.09800	0.04805	8.82663E-10	-1.86021E5
Cr	0.08300	0.07843	0.00136	-58918.48387
Ni	0.81900	0.87352	0.00250	-53474.75936
<b>Stable Phases</b>				
DIS_FCC_A1#1				
Moles	0.84221	Mass	46.67188	Volume Fraction 0.84210
Composition				
FCC_L12#2				
Moles	0.15779	Mass	8.35514	Volume Fraction 0.15790
Composition				
FCC_L12#2				
Mole Fraction	0.76668	Mass Fraction	0.84977	
Al	0.16698	0.08509		
Cr	0.06634	0.06514		

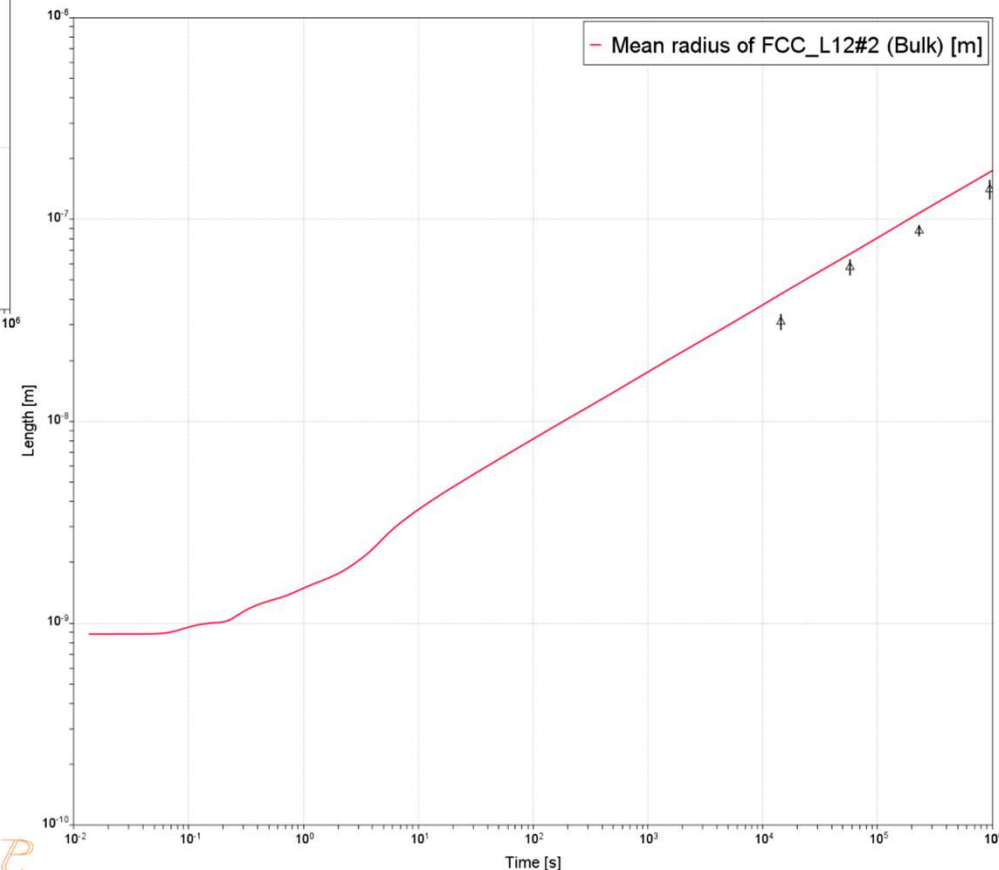
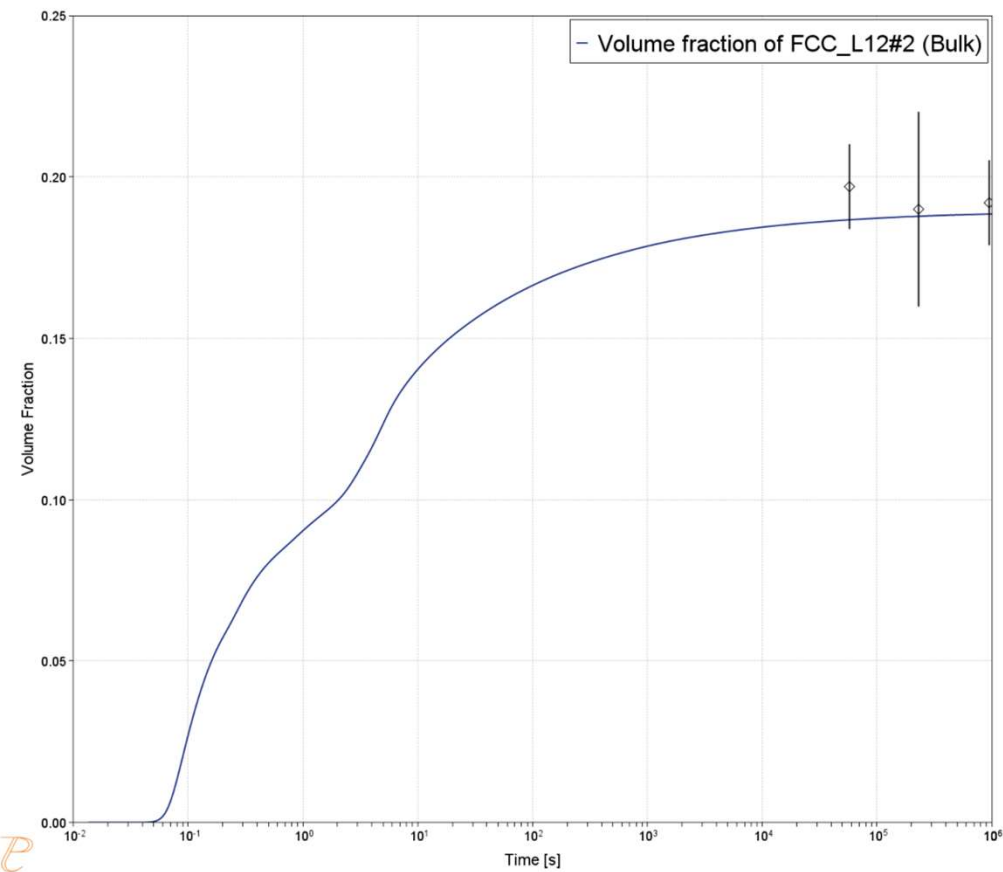
Also not a very good fit for mean radius as function of time.

# TC-PRISMA Example 1



System	
Database package	TCNI12 + MOBNI6
Elements	Ni, Al, Cr
Matrix phase	DIS_FCC_A1
Precipitate phases	FCC_L12#2
Conditions	
Composition	Ni – 9.8 Al – 8.3 Cr (at.%)
Temperature	800 °C
Simulation time	1E6 s
Nucleation properties	Nucleation Site Type: Bulk
Data Parameters – Interfacial Energies	
Interfacial Energy	Calculated
Molar Volume (Matrix phase):	DIS_FCC_A1: from database
Molar Volume (Precipitate phase):	FCC_L12#2: from database

# TC-PRISMA Example 1



Using Ni – 9.8 Al – 8.9 Cr (at-%)

## Influence of composition on monomodal versus multimodal $\gamma'$ precipitation in Ni-Al-Cr alloys

T. Rojhirunsakool · S. Meher · J. Y. Hwang ·  
S. Nag · J. Tiley · R. Banerjee

**Abstract** This study investigates the influence of alloy composition on  $\gamma'$  precipitation in Ni-8Al-8Cr and Ni-10Al-10Cr at.% during continuous cooling from a supersolvus temperature. When subjected to the same cooling rate, Ni-8Al-8Cr develops a monomodal population, whereas Ni-10Al-10Cr develops a multimodal (primarily bimodal) population of  $\gamma'$  precipitates. The bimodal  $\gamma'$  precipitate size distribution in Ni-10Al-10Cr alloy can be attributed to two successive nucleation bursts during continuous cooling while the monomodal  $\gamma'$  size distribution in Ni-8Al-8Cr results from a single nucleation burst followed by a longer time—wider temperature window for nucleation resulting in a larger number density of precipitates. Three-dimensional atom

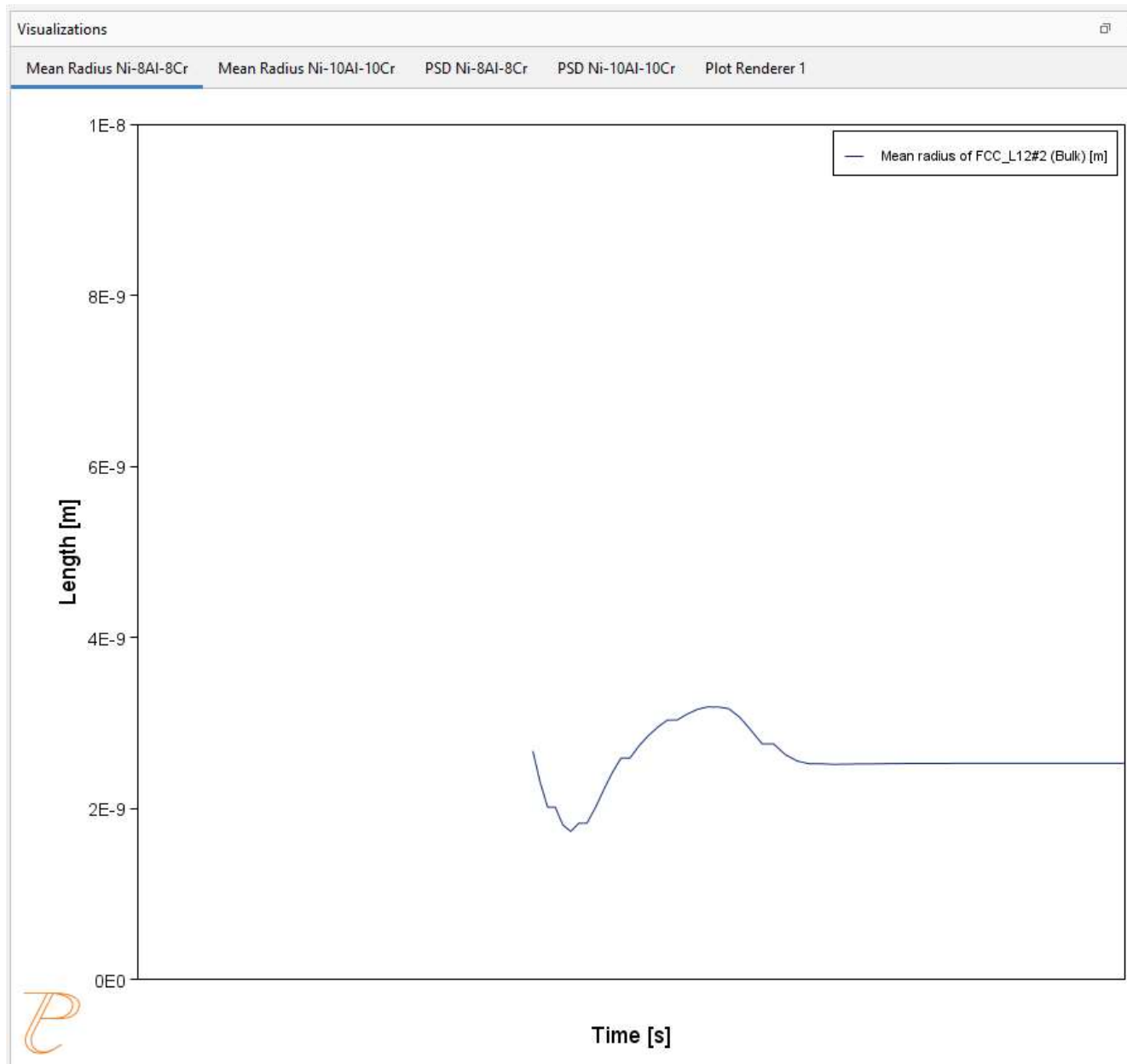
# Ni-alloy Example 2



System	
Database package	NIDEMO + MNIDEMO
Elements	Ni, Al, Cr
Matrix phase	DIS_FCC_A1
Precipitate phases	FCC_L12#2
Conditions	
Composition	Ni – 10 (8) Al – 10 (8) Cr (at.%)
Temperature	940 - 380 °C
Simulation time	2400 s
Nucleation properties	Nucleation Site Type: Bulk
Data Parameters – Interfacial Energies	
Interfacial Energy	Bulk: 0.023 J/m <sup>2</sup>
Molar Volume (Matrix phase):	DIS_FCC_A1: from database
Molar Volume (Precipitate phase):	FCC_L12#2: from database
Mobility Enhancement Factor	1 (i.e. no change)

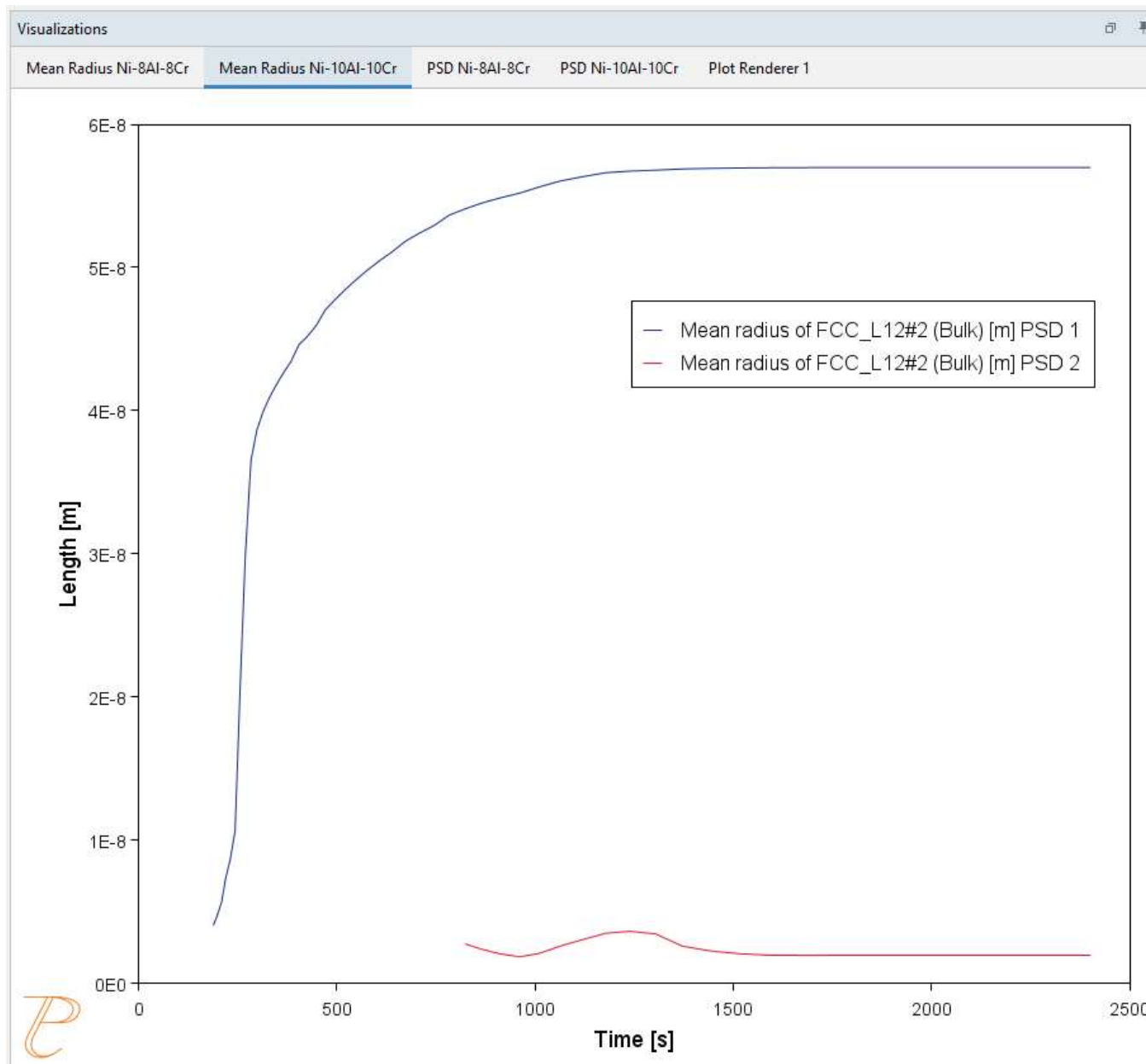
# Ni-alloy Example 2

Ni – 8 Al – 8 Cr



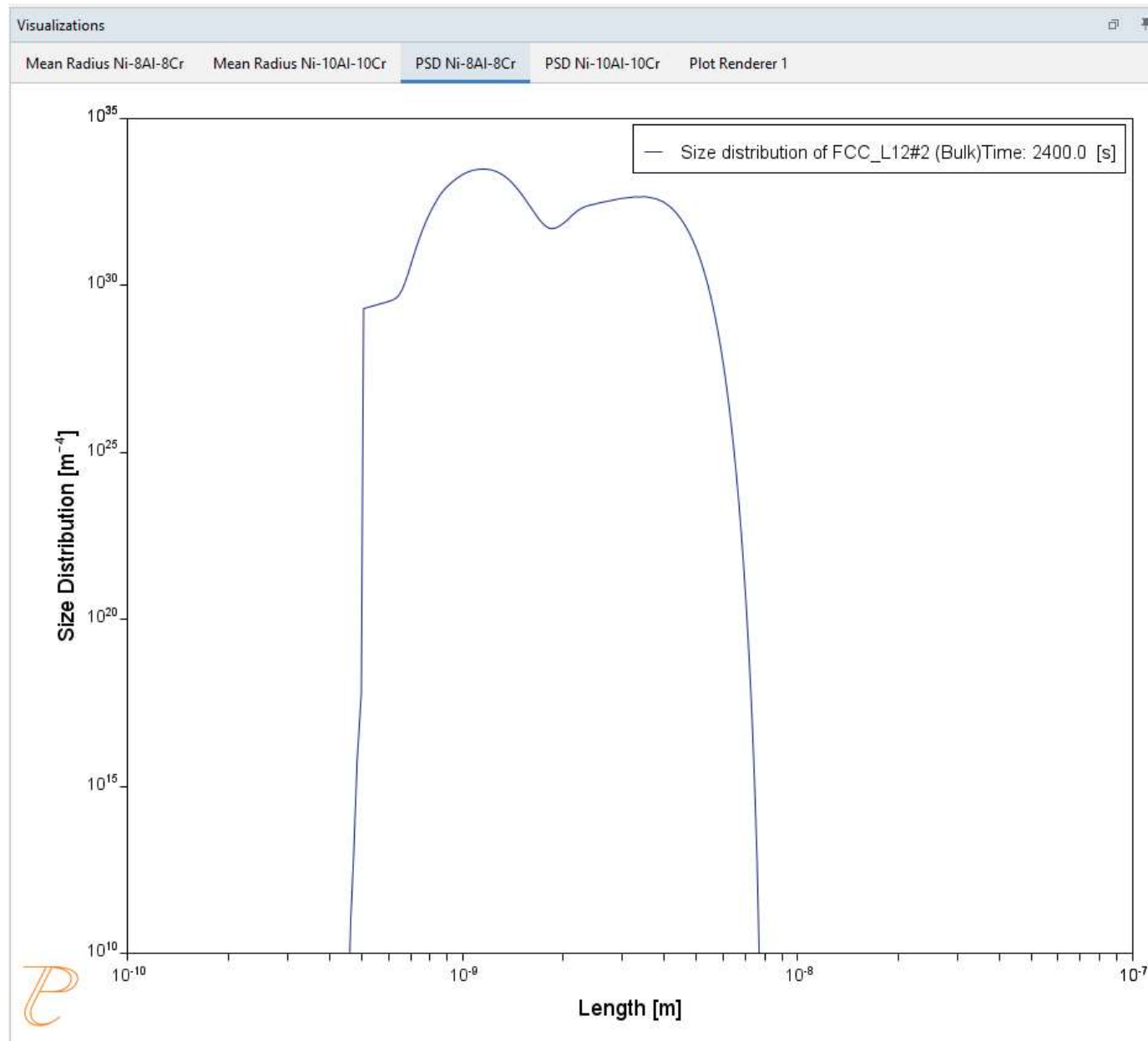
# Ni-alloy Example 2

Ni – 10 Al – 10 Cr



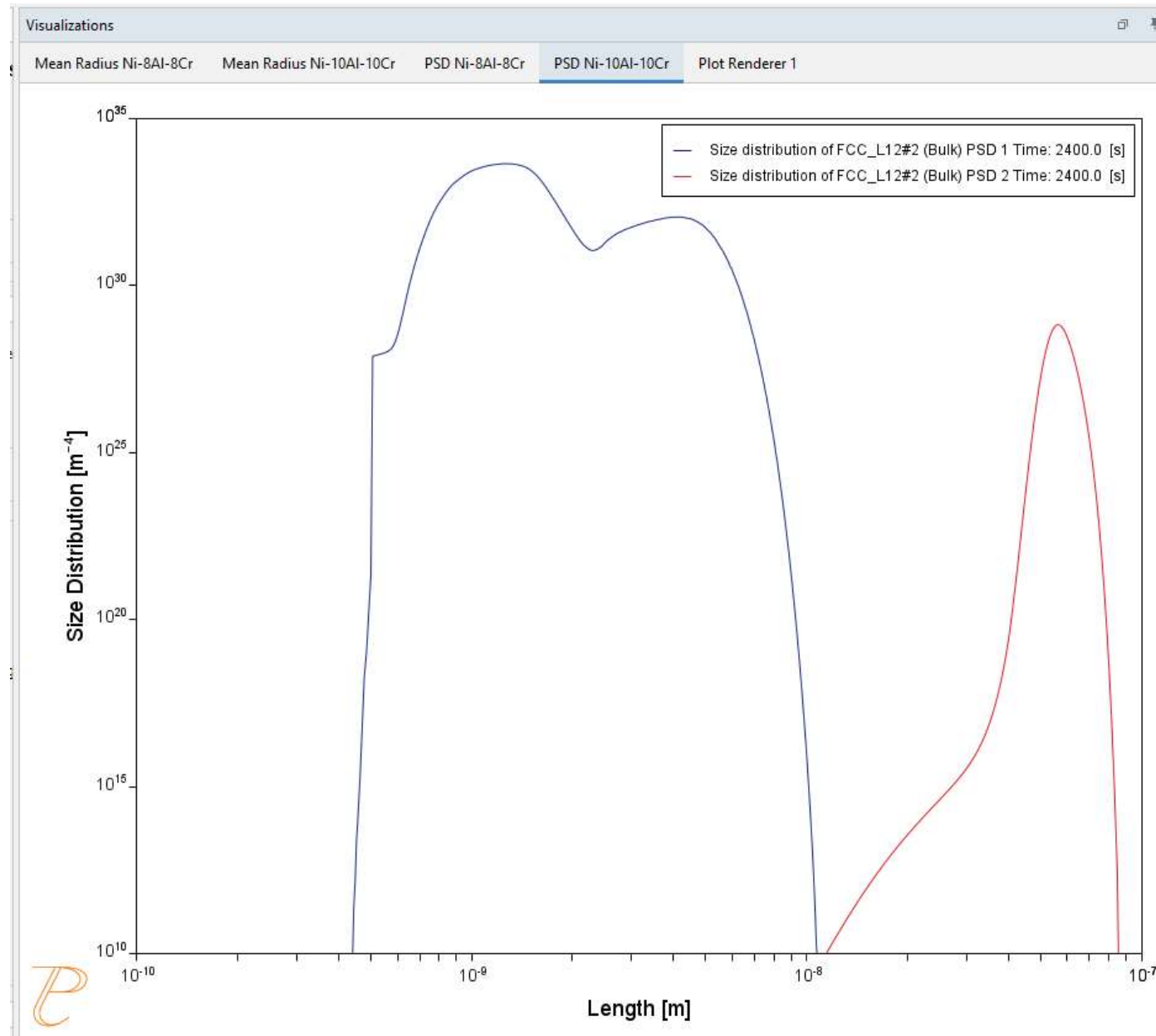
# Ni-alloy Example 2

Ni – 8 Al – 8 Cr



# Ni-alloy Example 2

Ni – 10 Al – 10 Cr

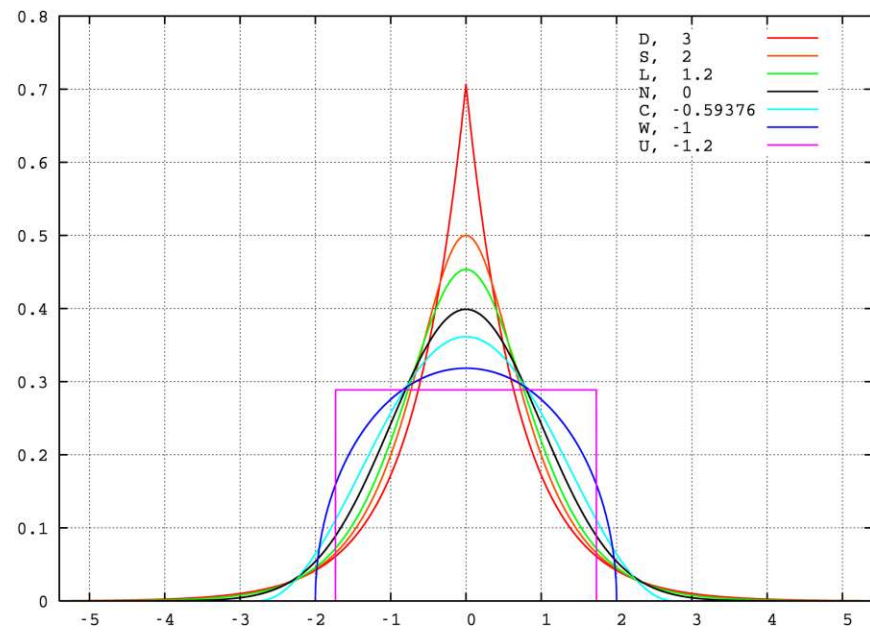


# Parameters for Multi-Modal Distribution

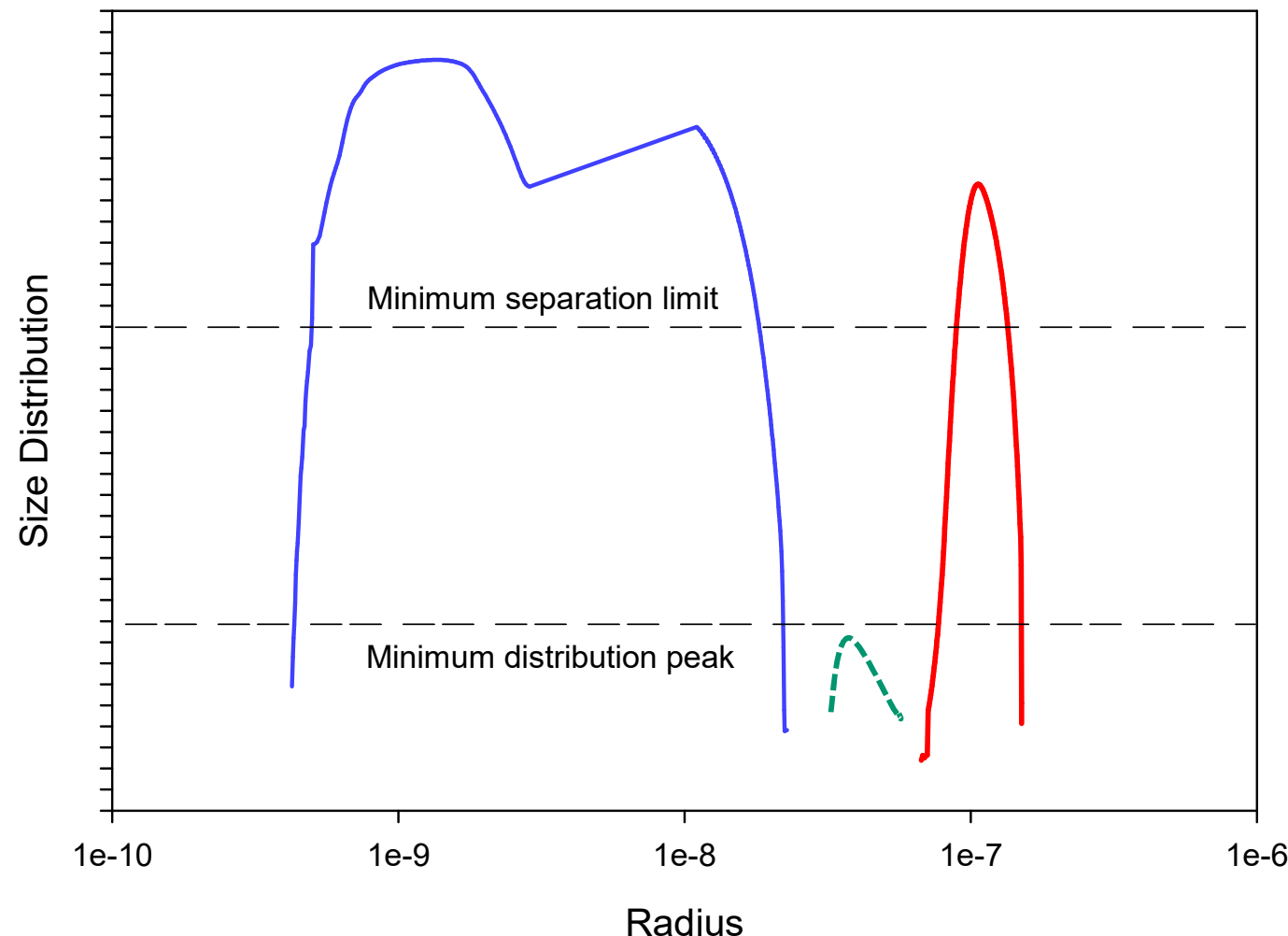
- Kurtosis
  - ✓ Measurement of Peakedness
- Excess Kurtosis

$$\gamma_2 = \frac{\frac{1}{n} \sum_{i=1}^n (x_i - \bar{x})^4}{\left( \frac{1}{n} \sum_{i=1}^n (x_i - \bar{x})^2 \right)^2} - 3$$

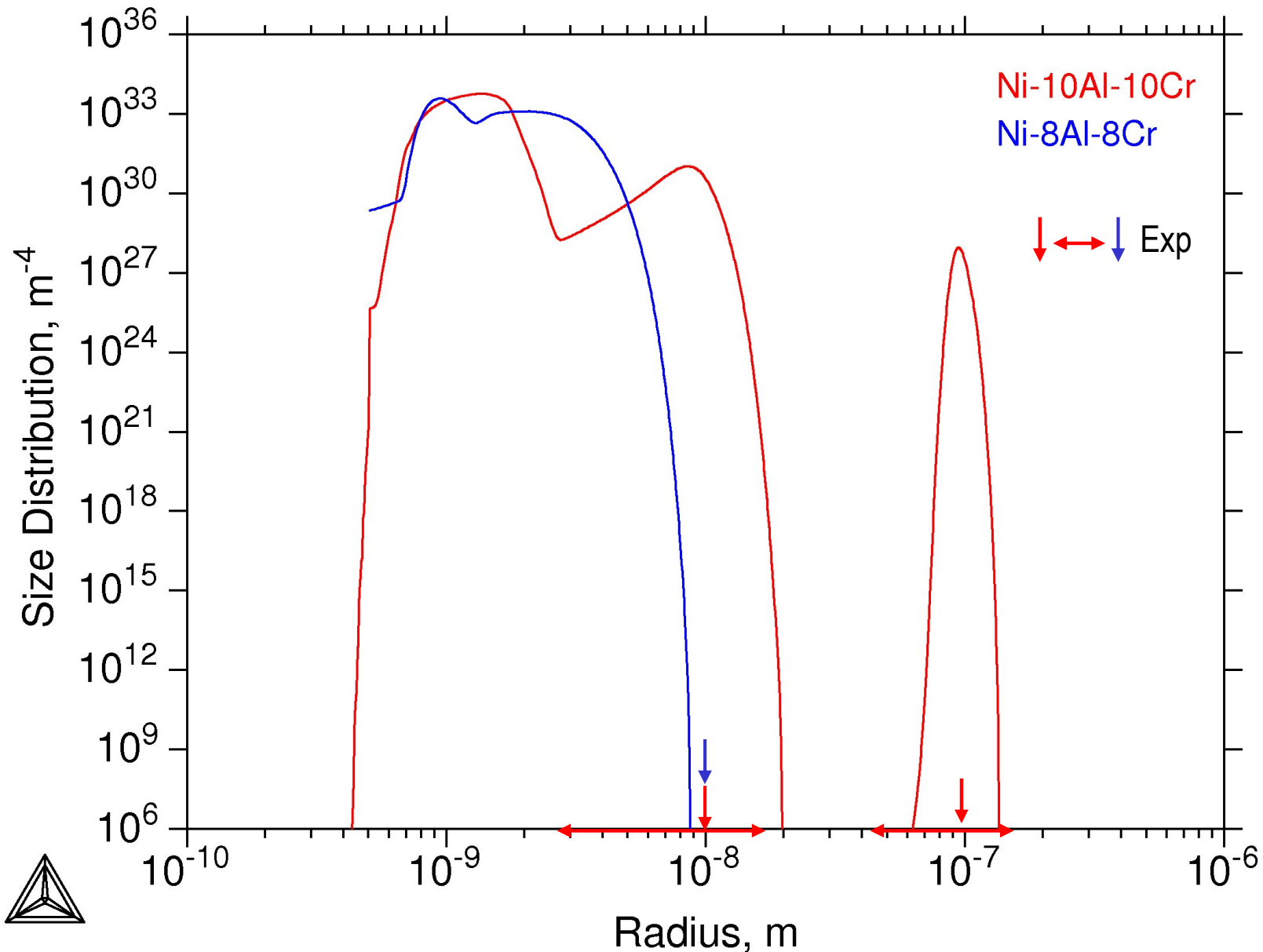
- ✓ Larger excess kurtosis, more distribution on peak and tail



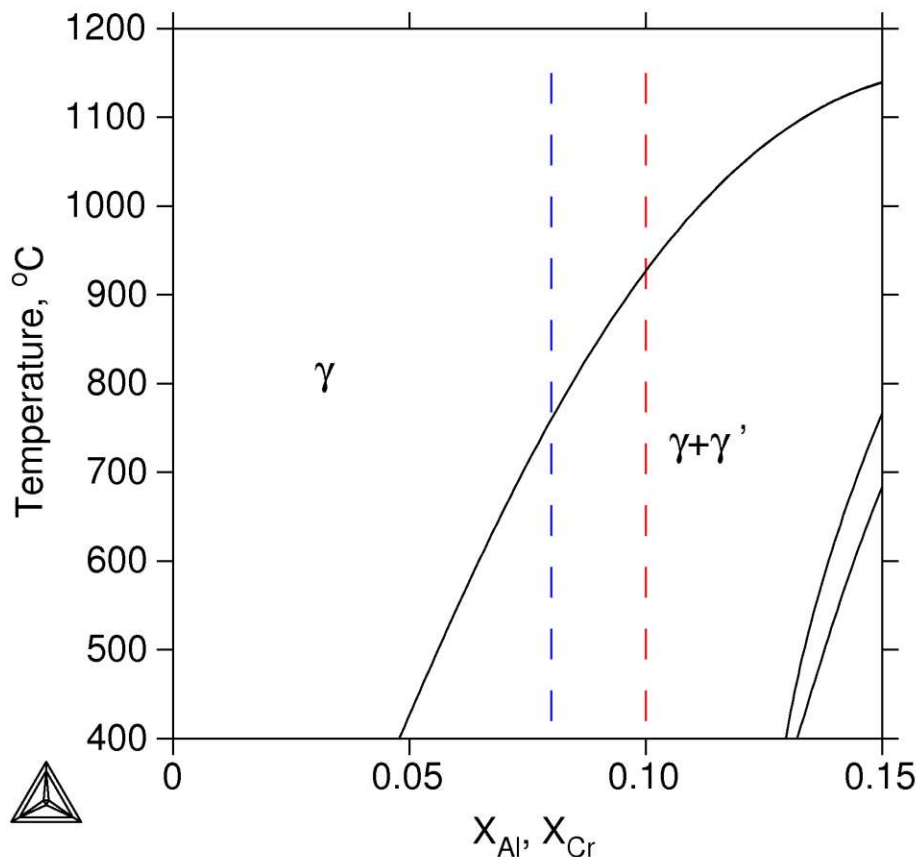
# Parameters for Multi-Modal Distribution



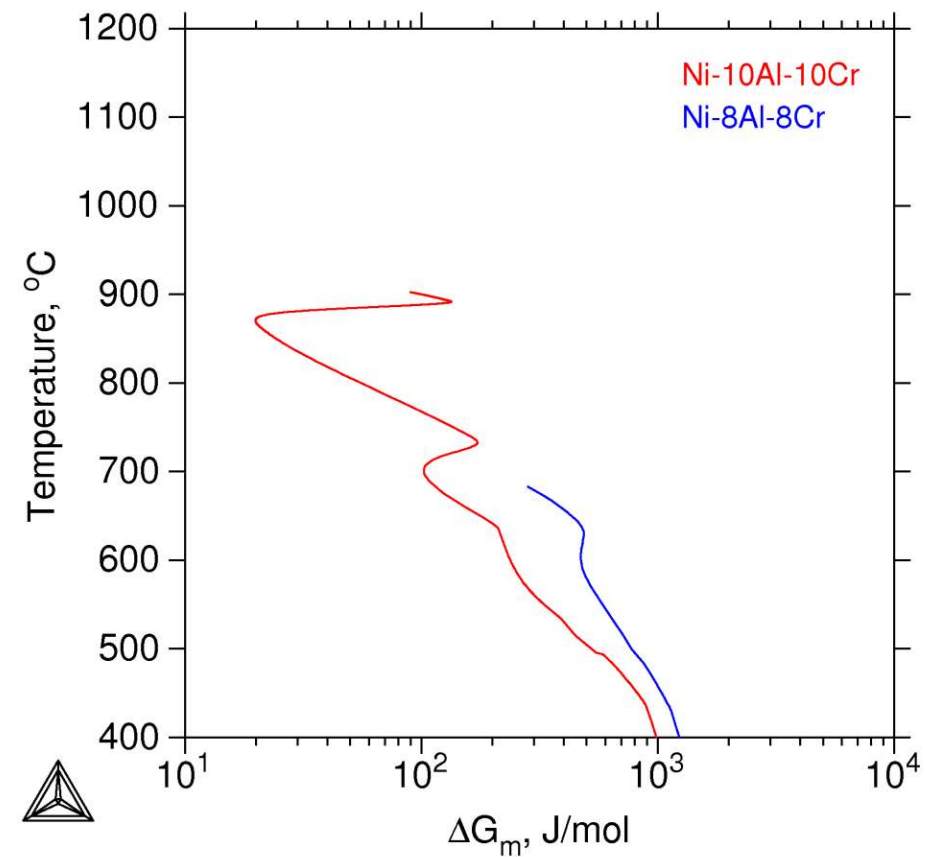
# Ni-10Al-10Cr and Ni-8Al-8Cr



# Ni-10Al-10Cr and Ni-8Al-8Cr

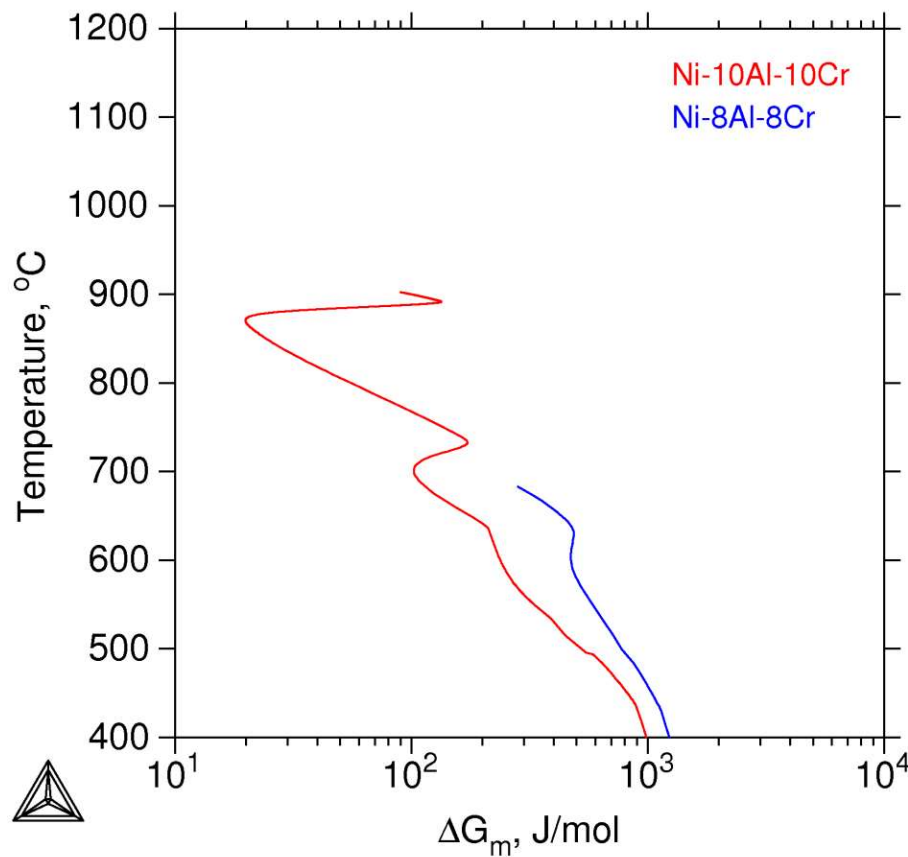


Vertical phase diagram  
section in Ni-xAl-xCr

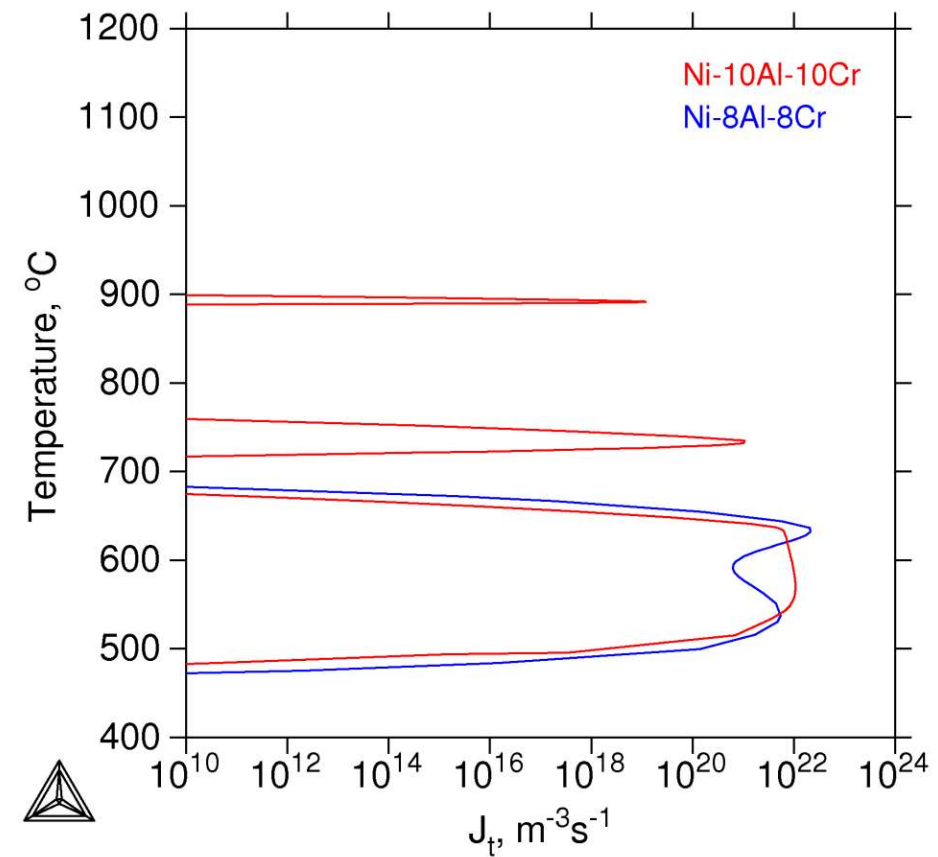


Thermodynamic driving force

# Ni-10Al-10Cr and Ni-8Al-8Cr



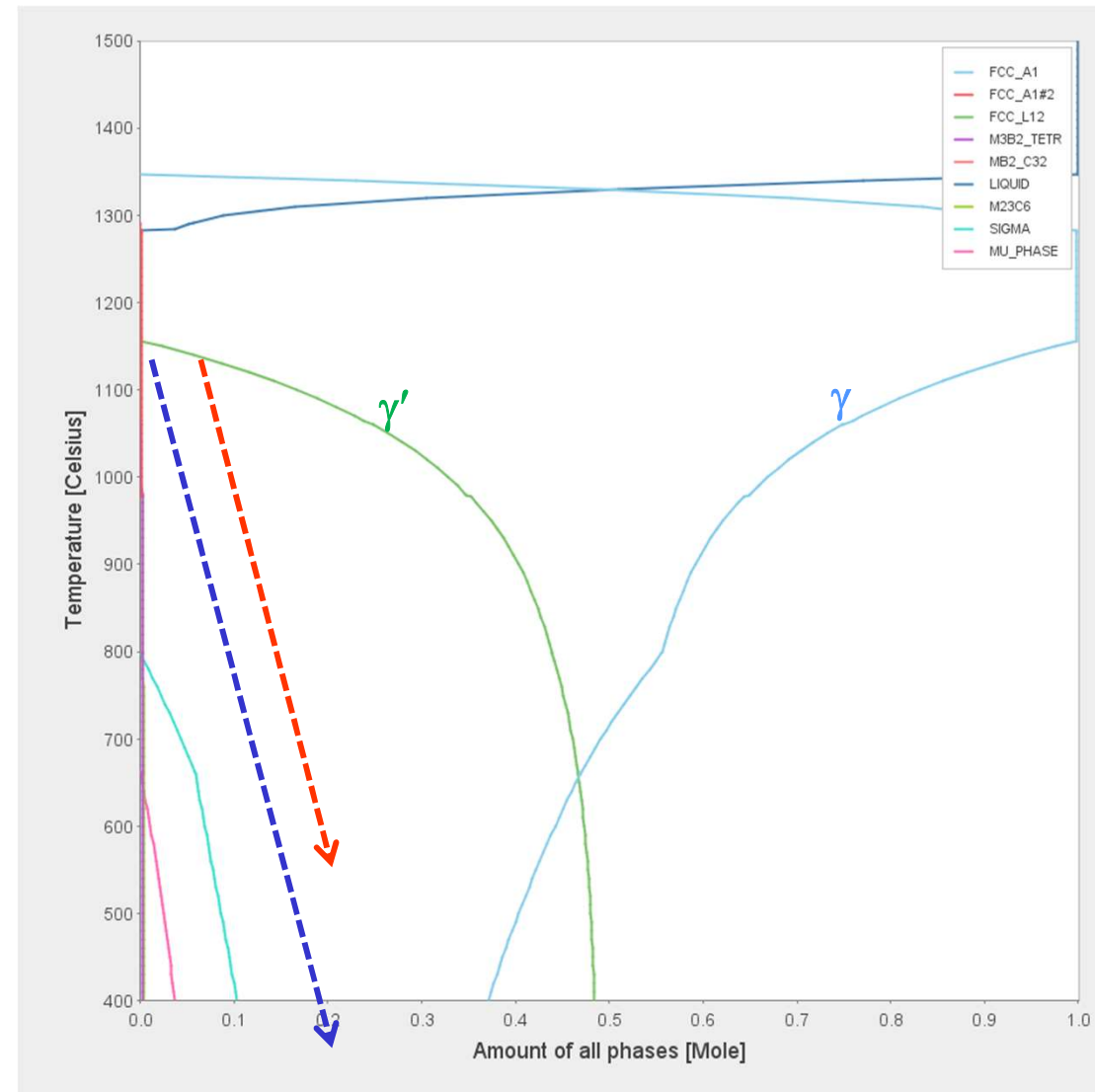
Thermodynamic driving force



Nucleation rate

## Precipitation Kinetics during Continuous Cooling

wt.%	1*	2**
Al	2.53	2.46
B	0.014	
C	0.014	0.025
Co	14.43	14.75
Cr	15.92	16.35
Fe	0.09	0.06
Mo	2.96	3.02
Ti	4.96	4.99
W	1.26	1.3
Zr		0.035
Ni	Bal	Bal



➤ Databases: TTNI8+MOBNI1

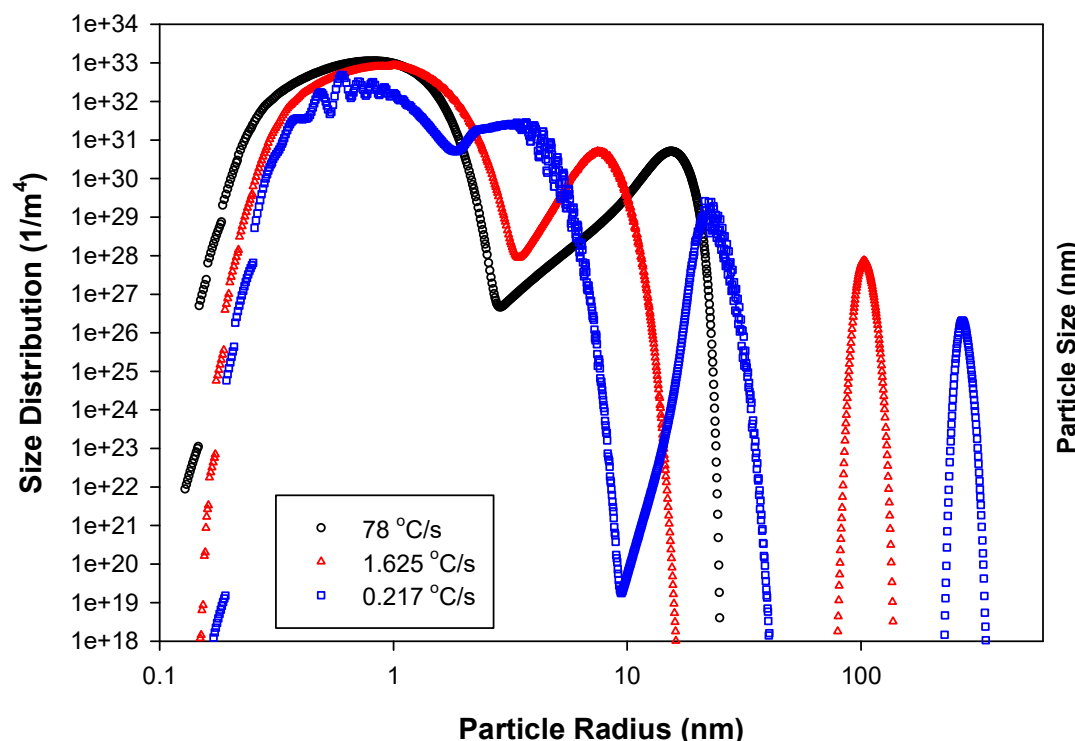
\* Radis et al., *Superalloys 2008*

\*\* Mao et al., *Metall. Mater. Trans. A, 32A(10) 2441(2001)*

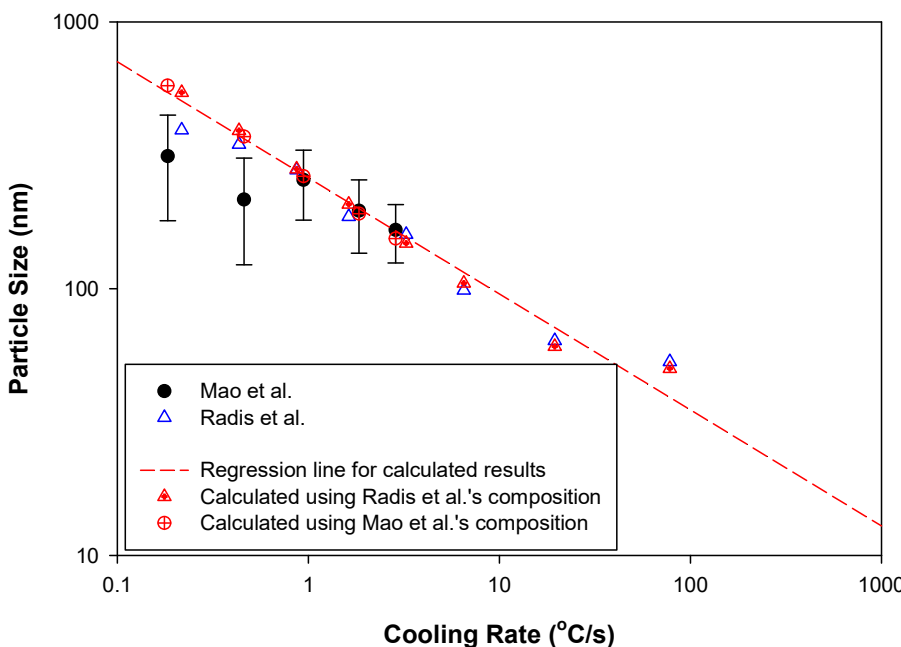
# U720Li : Cooling Rate Effect



## Size Distribution



## Mean Particle Size



## Co-Precipitation of $\gamma'$ and $\gamma''$ from FCC ( $\gamma$ ) ---

Complex example to try on your own.

$\gamma'$  FCC L1<sub>2</sub>

Chemical Composition (wt.%)\*

Fe	Cr	Nb	Mo	Al	Ti	Ni
18.14	17.9	5.3	2.99	0.5	0.97	Bal.

$\gamma''$  BCT DO<sub>22</sub>  
 $(001)_{\gamma''} \parallel \{001\}_{\gamma}$   
 $[100]_{\gamma''} \parallel <100>_{\gamma}$

- $\gamma'$  : Sphere +  $\gamma''$  : Plate
- $\gamma'$  misfit strain from database
- $\gamma''^*$  :

---

Coherency strains  $\varepsilon$

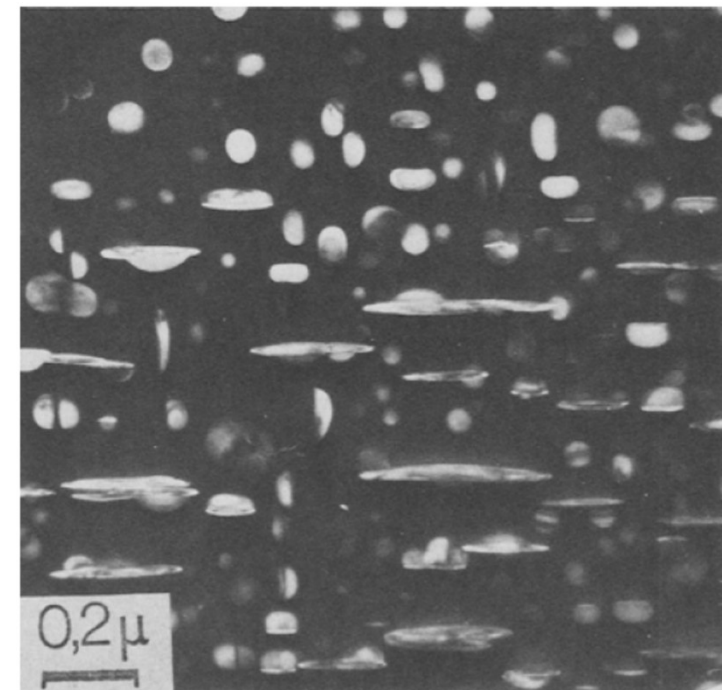
$$\varepsilon_{11}^T = 6.67 \times 10^{-3}$$
$$\varepsilon_{33}^T = 2.86 \times 10^{-2}$$

Shear modulus at 1223 K

$$\mu = 57.1 \text{ GPa}$$

Poisson's ratio

$$\nu = 0.33$$

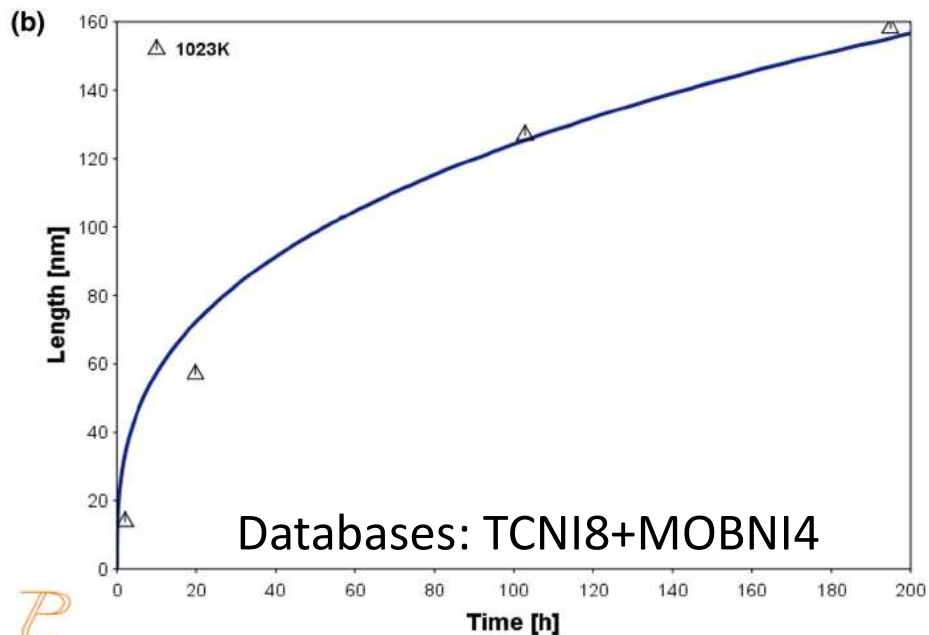


\* A. Devaux et al. *Mater. Sci. Eng. A* 486(2008)117

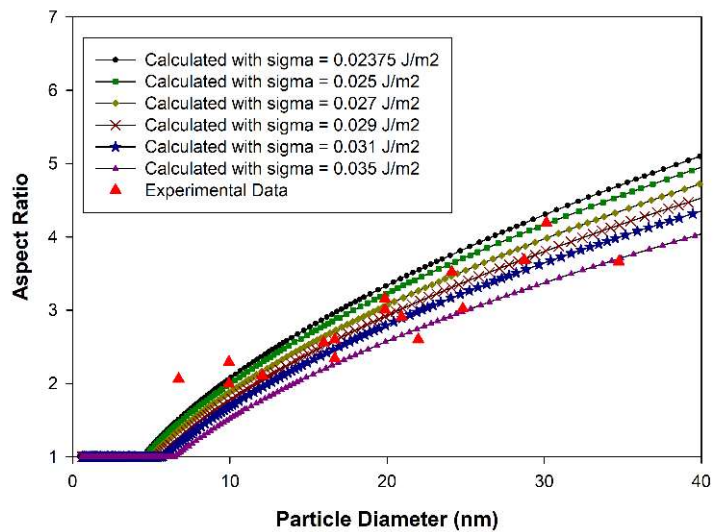
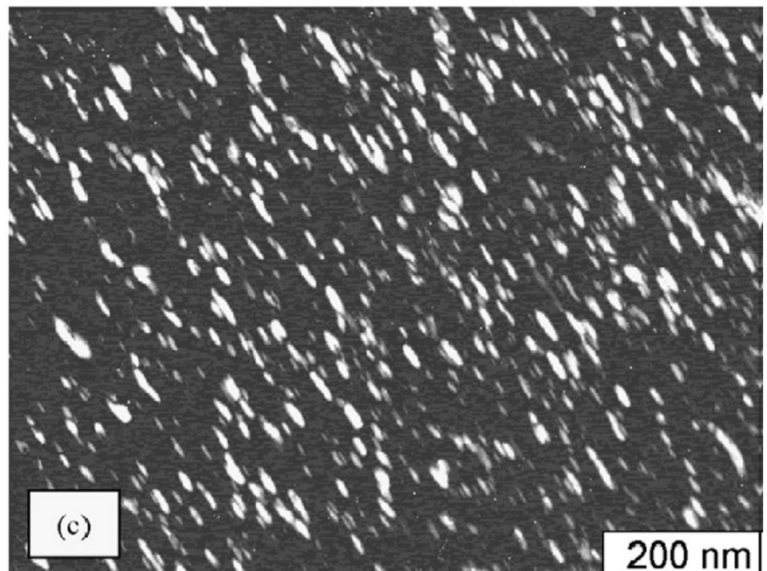
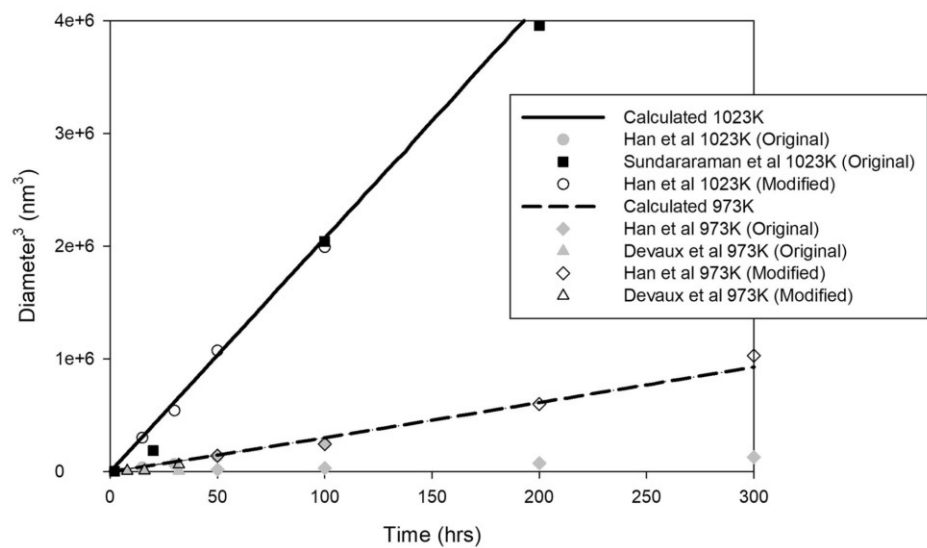
\*\* R. Cozar and A. Pineau, *Metall Trans. B* 4(1973)47

**Microstructure of IN718\*\***

# Results - IN718 example



P



\* Experimental Data and Picture from A. Devaux et al. *Mater. Sci. Eng. A* 486(2008)117; M. Sundararaman et al., *Met. Trans. A*, 23(1992)2015

# Q & A

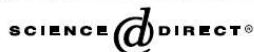
# Examples

## Steel

# Multi-precipitates



Available online at [www.sciencedirect.com](http://www.sciencedirect.com)



Acta Materialia 53 (2005) 519–531



[www.actamat-journals.com](http://www.actamat-journals.com)

## Simulation of the kinetics of precipitation reactions in ferritic steels

A. Schneider \*, G. Inden

Department of Materials Technology, Max-Planck-Institut für Eisenforschung GmbH, Max-Planck-Straße 1, 40237 Düsseldorf, Germany

Received 15 June 2004; received in revised form 1 October 2004; accepted 4 October 2004

Available online 5 November 2004

### Abstract

Computer simulations of diffusion-controlled phase transformations in model alloys of Fe–Cr–C, Fe–Cr–W–C, Fe–Cr–Si–C, and Fe–Cr–Co–V–C are presented. The compositions considered are typical for ferritic steels. The simulations are performed using the software DICTRA and the thermodynamic calculations of phase equilibria are performed using Thermo-Calc. The thermodynamic driving forces and the kinetics of diffusion-controlled precipitation reactions of  $M_{23}C_6$ ,  $M_7C_3$ , cementite and Laves-phase (Fe, Cr)<sub>2</sub>W are discussed. The simultaneous growth of stable and metastable phases is treated in a multi-cell approach. The results show remarkable effects on the growth kinetics due to the competition during simultaneous growth.

© 2004 Acta Materialia Inc. Published by Elsevier Ltd. All rights reserved.

**Keywords:** Ferritic steels; Phase transformation kinetics; Thermodynamics; Kinetics

A. Schneider, G. Inden / *Acta Materialia* 53 (2005) 519–531

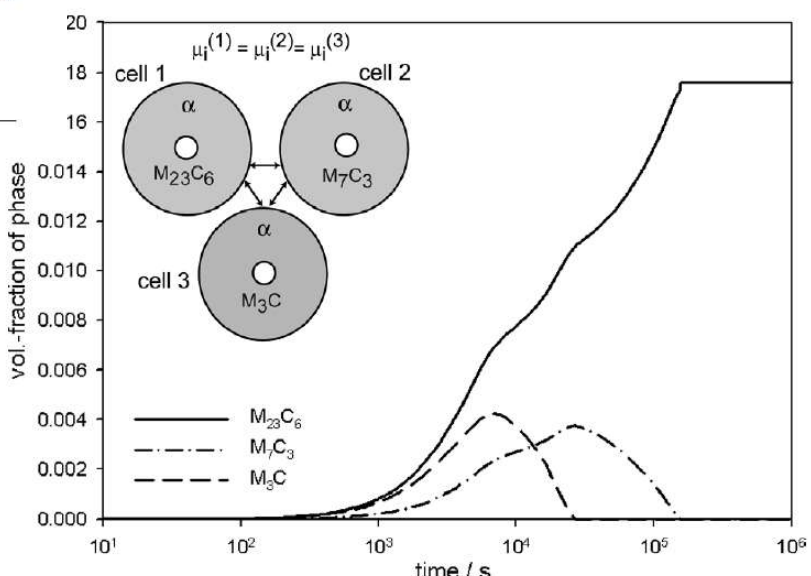


Fig. 6. Three-cell simulation of competitive growth of stable  $M_{23}C_6$  and of metastable  $M_7C_3$  and  $M_3C$  in Fe–12Cr–0.1C at 1053 K. Nucleus sizes were 5  $\mu\text{m}$  and the nucleus sizes were 1 nm in each cell.

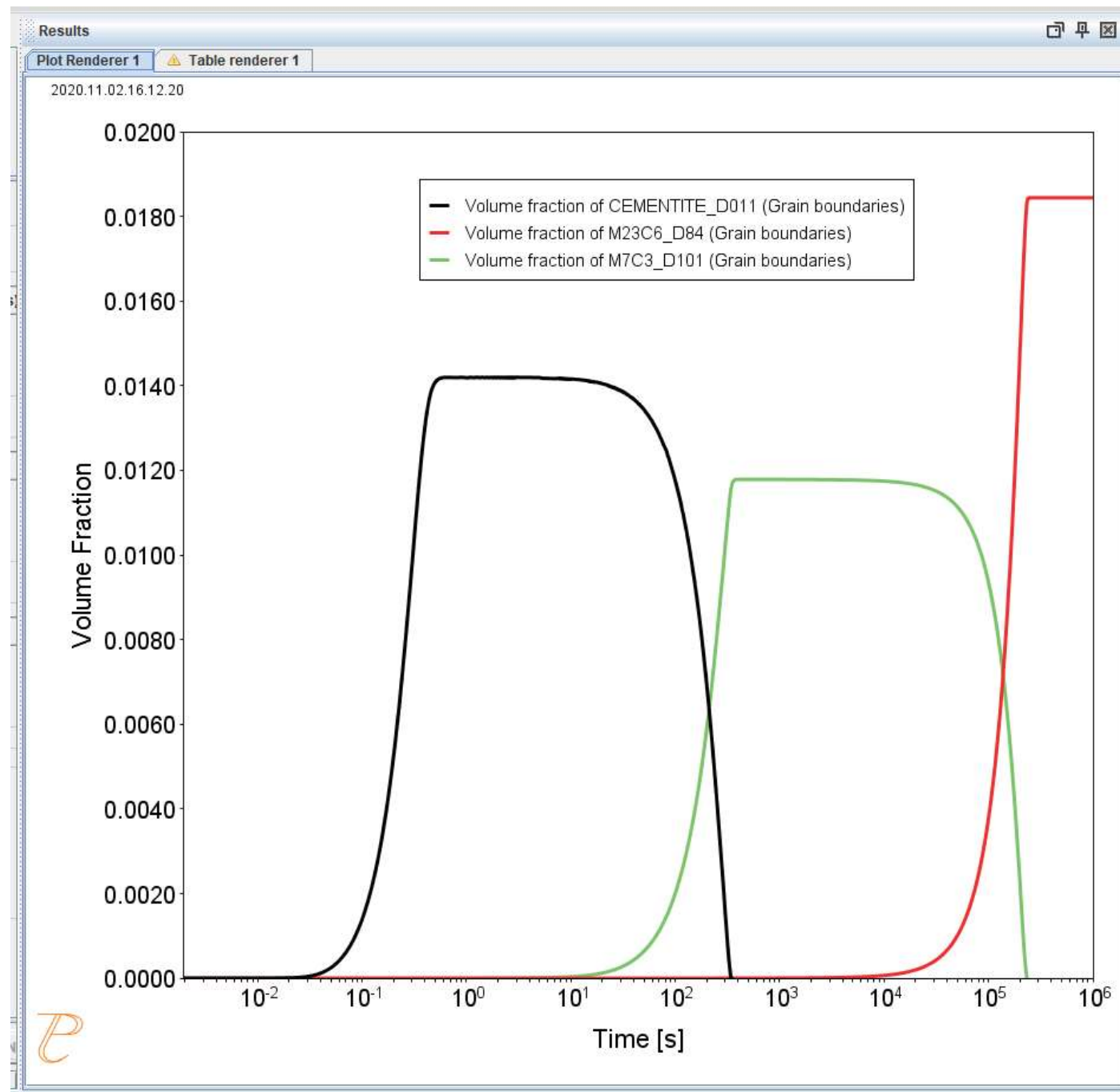
# Steel Example 1



System	
Database package	TCFE13 + MOBFE8
Elements	Fe, Cr, C
Matrix phase	Bcc_A2
Precipitate phases	$M_{23}C_6$ , $M_7C_3$ , Cementite
Conditions	
Composition	Fe – 12 Cr – 0.1 C (wt.%)
Temperature	1053 K
Simulation time	1e6 s
Nucleation properties	Nucleation Site Type: Grain Boundaries
Data Parameters–Interfacial Energies	
Cementite	0.167 J/m <sup>2</sup>
$M_{23}C_6$	0.252 J/m <sup>2</sup>
$M_7C_3$	0.282 J/m <sup>2</sup>

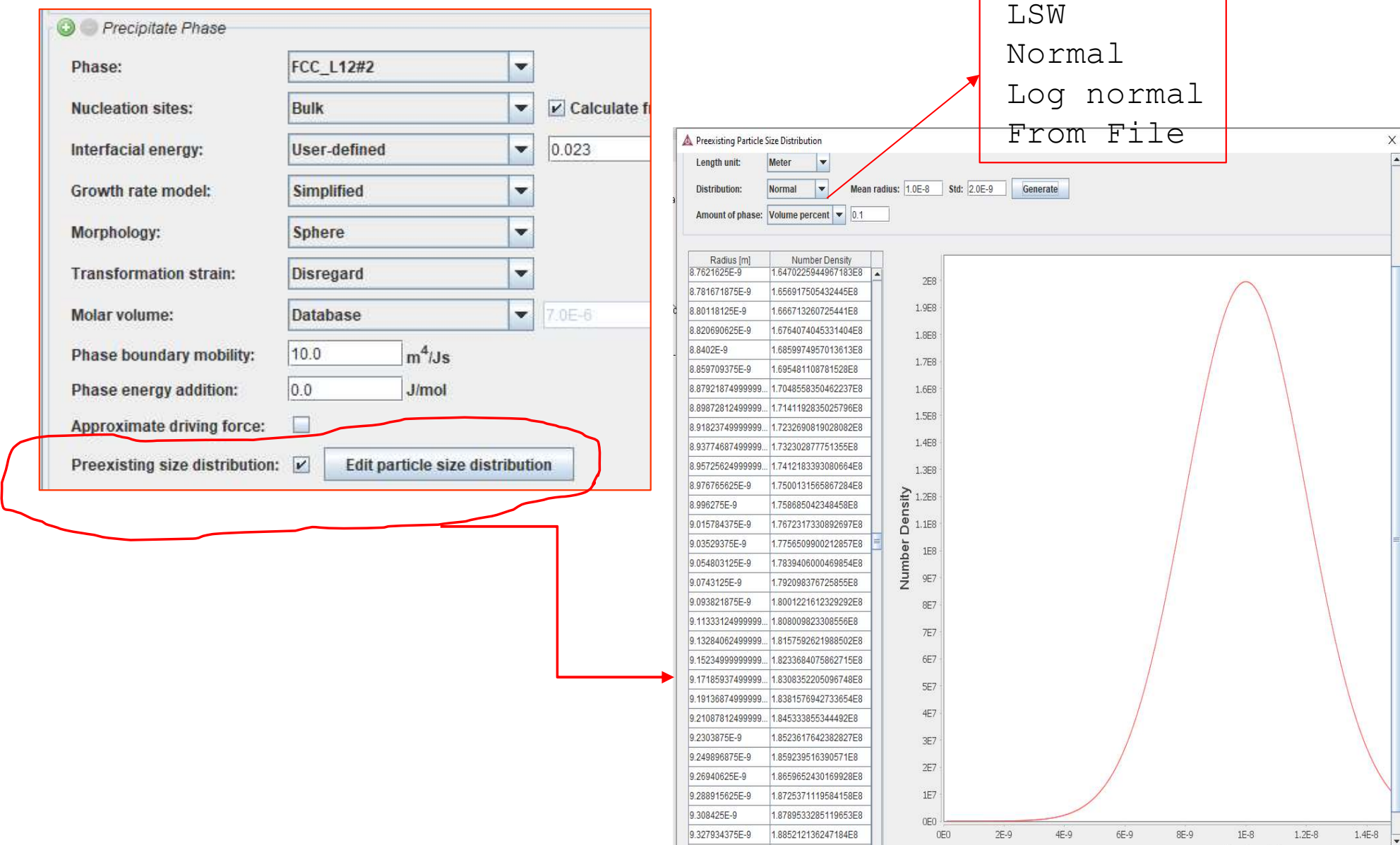
To include already existing size distributions – see Example 2

# Steel Example 1



# Steel Example 2

Same as Ex 1 but starting from already existing particle distributions of all three carbides, with small mean radius.

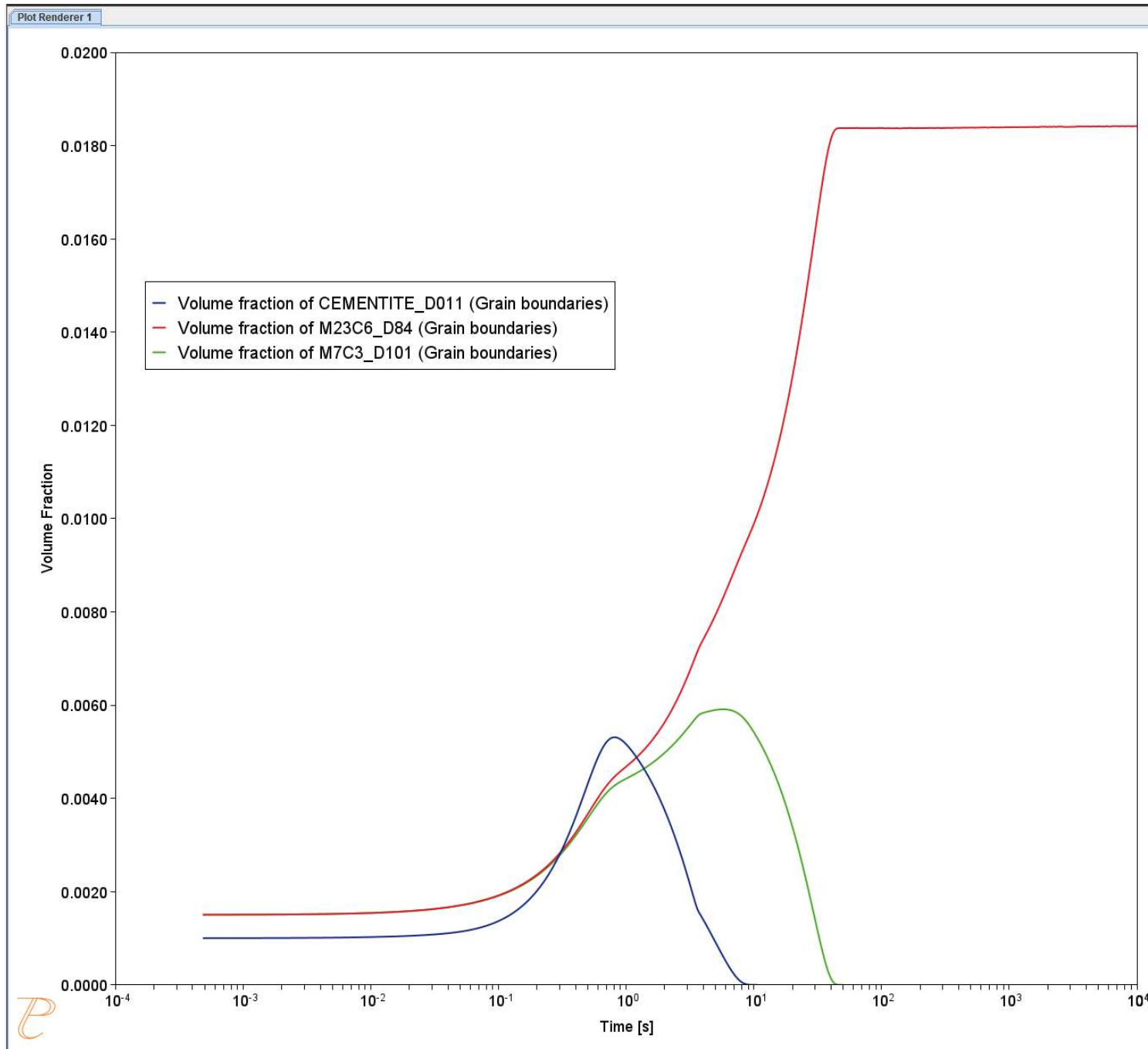


# Steel Example 2



Initial Particle Size Distribution	
Phase	CEMENTITE
Initial composition	Cr 71.4 wt.%
Distribution	LSW with mean radius 1.0e-8m
Amount	0.001 (volume fraction)
Initial Particle Size Distribution	
Phase	M23C6
Initial composition	Cr 69.3 wt.%
Distribution	LSW with mean radius 1.0e-8m
Amount	0.0015 (volume fraction)
Initial Particle Size Distribution	
Phase	M7C3
Initial composition	Cr 82.9 wt.%
Distribution	LSW with mean radius 1.0e-8m
Amount	0.0015 (volume fraction)

# Steel Example 2

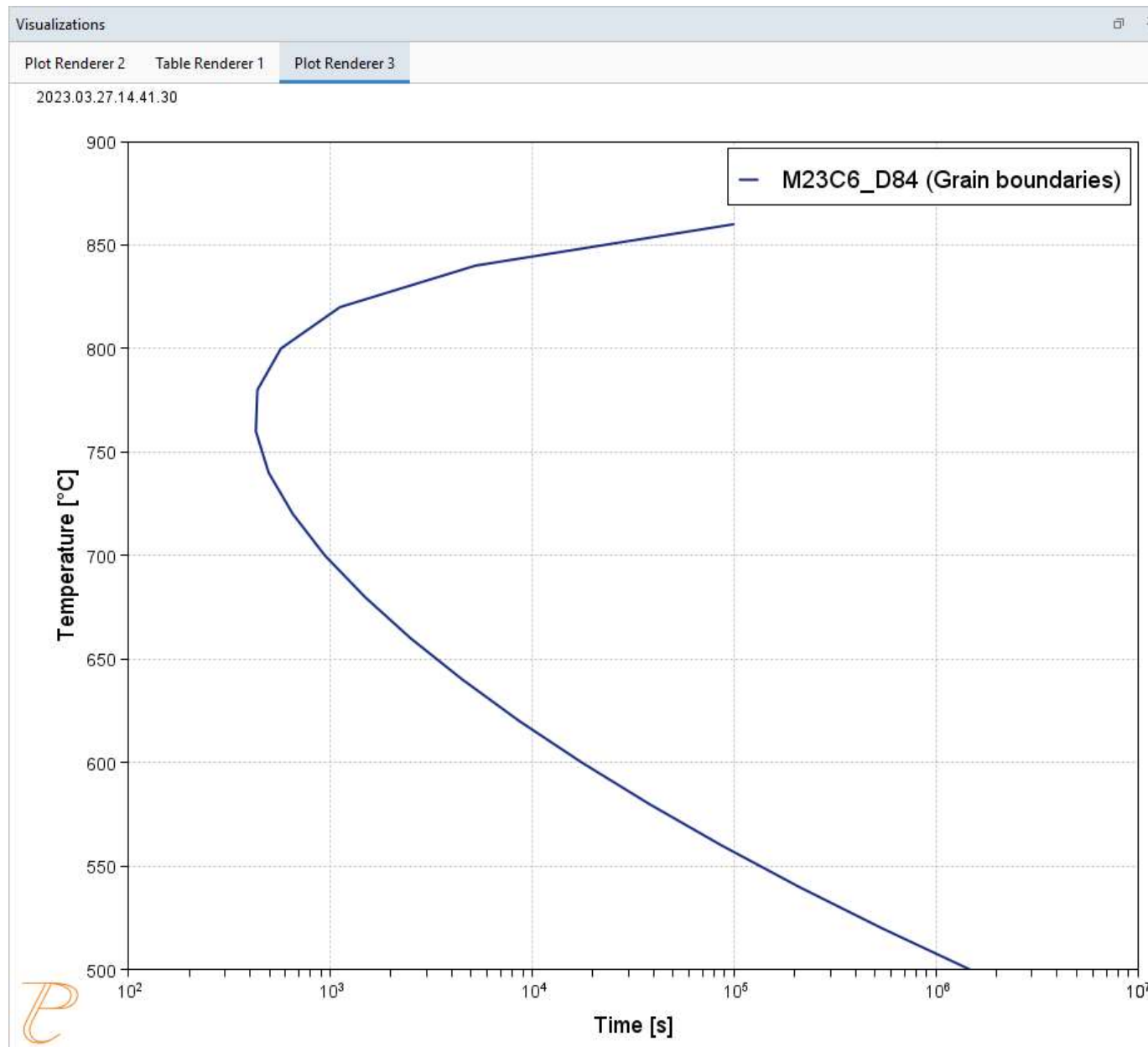


# Steel Example 3 – TTP



System		
Database package	TCFE13 + MOBFE8	
Elements	Fe,C,Cr,Mn,Ni,Si	
Matrix phase	Fcc_A1	Number of grid points: 15 Maximum number of grid points: 20 Minimum number of grid points: 10
Precipitate phase	M <sub>23</sub> C <sub>6</sub>	
Conditions – TTT diagram	- Phase fraction = 0.001	
Composition	Fe-0.068C-20.89Cr-1.61Mn-10.28Ni-0.49Si (wt.%)	
Temperature	500 °C, 860 °C, 20 °C	
Simulation time	1E7 s	
Nucleation properties	Nucleation Site Type: Grain Boundary, Grain size 100 µm	
Data Parameters		
Interfacial Energy	Grain Boundary: Calculated	

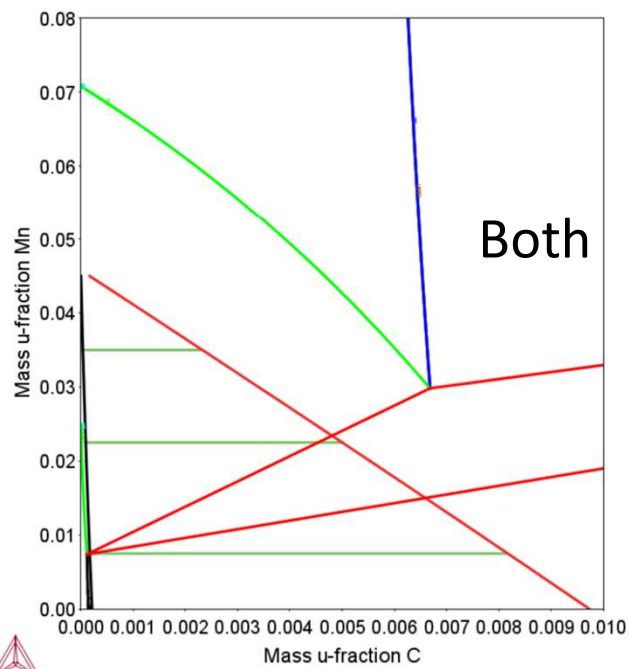
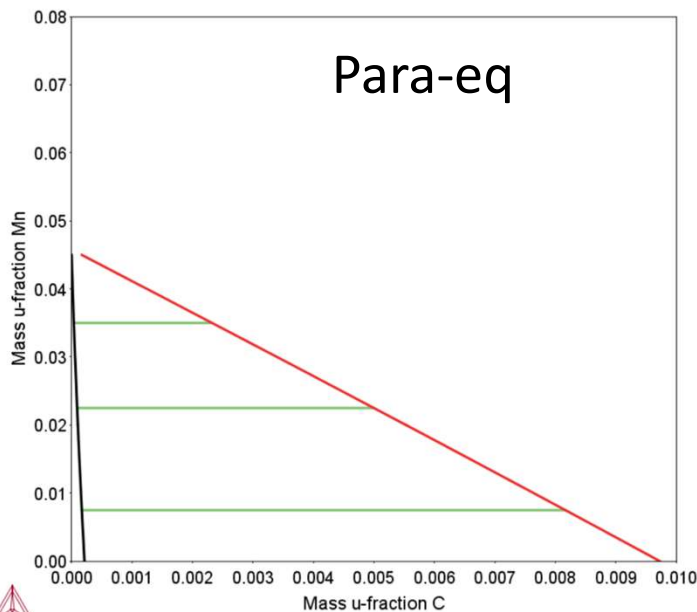
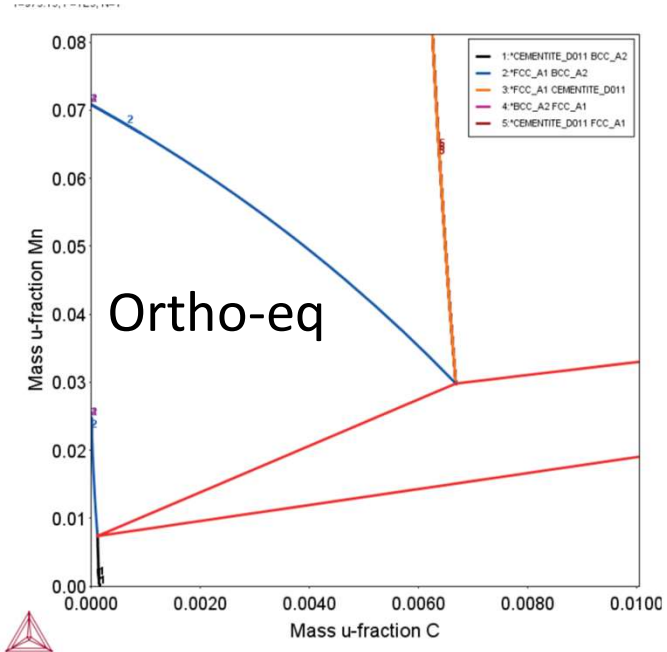
# Steel Example 3



# Example

# Para-Equilibrium

# Para-equilibrium



Bcc + Fcc equilibria  
in Fe – Mn – C

# Example: Para-equilibrium or not?

Precipitation of cementite during tempering of martensite in a Fe-Mn-C steel.

Consider three different interface conditions: the usual ortho-equilibrium condition, para-equilibrium condition, and a smooth transition from para-equilibrium to ortho-equilibrium condition using the new ***PE Automatic*** growth rate model.

The simulation results can be compared with the experimental data from Miyamoto et al. [2007Miy].

Martensite will be represented by BCC\_A2 which requires some considerations about mobility and also grain size and grain shapes.

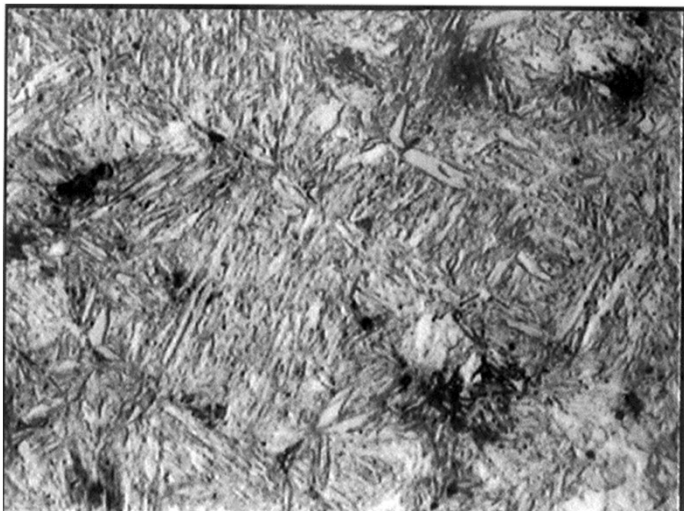


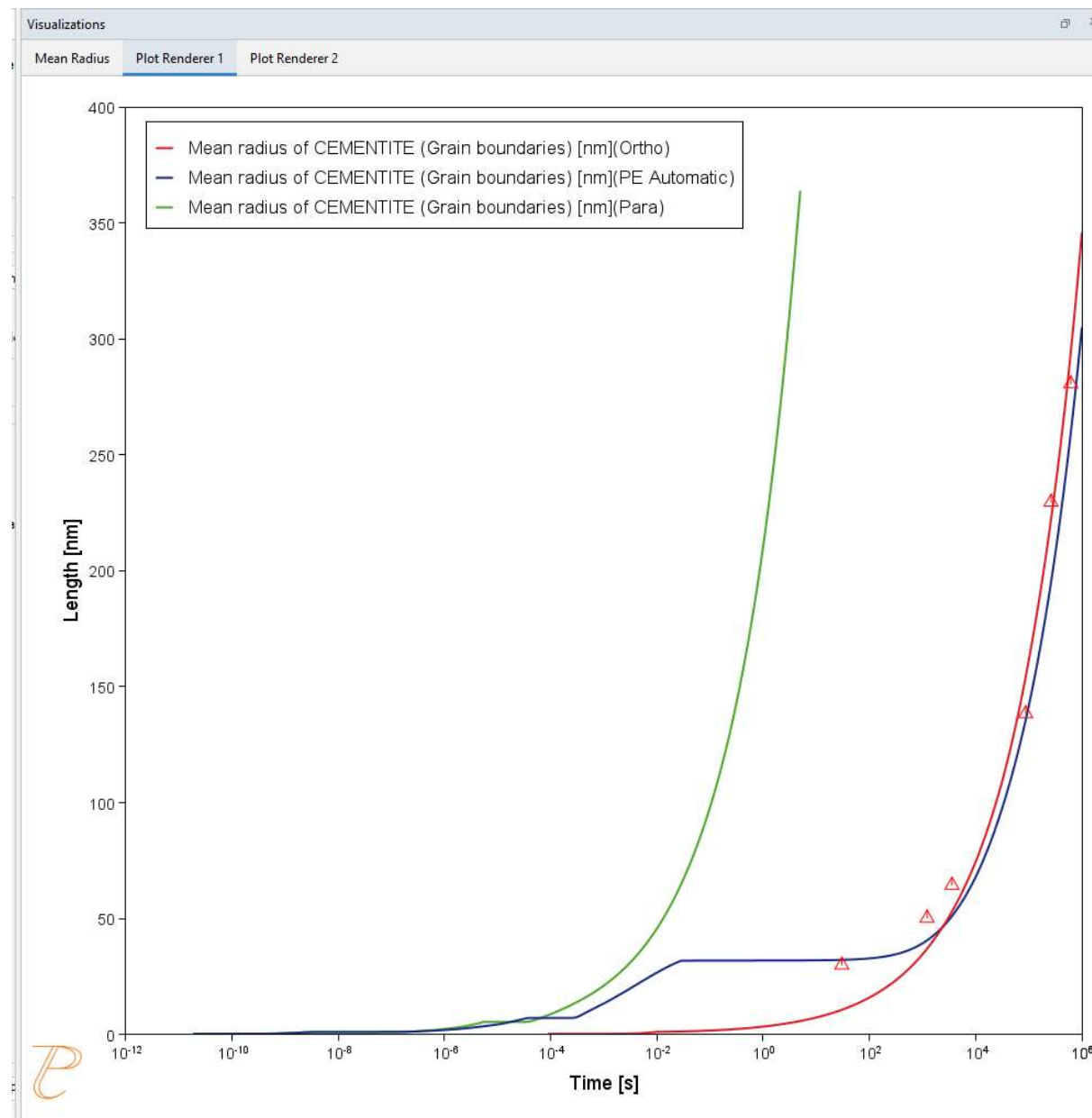
Image from Wikipedia

[2007Miy] G. Miyamoto, J. Oh, K. Hono, T. Furuhara, T. Maki, Effect of partitioning of Mn and Si on the growth kinetics of cementite in tempered Fe–0.6 mass% C martensite. *Acta Mater.* 55, 5027–5038 (2007).

# Example – Para-equilibrium or not?

<b>System</b>	
Database package	TCFE13 + MOBFE8
Elements	Fe, Mn, C
Matrix phase	BCC_A2
Precipitate phase	Cementite
<b>Conditions</b>	
Composition	Fe- 0.61 C- 1.96 Mn (wt-%)
Temperature	650 °C
Simulation time	1E6 s (5 s for PE)
Growth rate models	Simplified / Para-eq / PE Automatic
Nucleation properties	Nucleation Site: Grain boundaries
<b>Data Parameters</b>	
Interfacial Energy	Calculated
Molar Volumes	Database
Grain size / Grain aspect ratio	1E-7 m / 100
Mobility Adjustment factor	0.008
Activation energy	- 70000 J/mol

# Example – Para-equilibrium or not?



Link to course evaluation:

<https://www.surveymonkey.com/r/6KWGXN9>

We will send a **course certificate** by email within  
the next few days.

Email [ake@thermocalc.se](mailto:ake@thermocalc.se) if you think we have  
your name and affiliation incorrect.

# Q & A